NUST INSTITUTE OF CIVIL ENGINEERING

B.E Civil Engineering Batch 2009 Final Year Project Report on

Demonstration of Liquefaction by Construction of Liquefaction Tank & Study of its Mitigation Method

Submitted by:

Waleed Hasan (Group Leader)	**BE-CE-2009-140**
Abu Bakr Jamil	BE-CE-2009-149
Jawad Mughal	BE-CE-2009-61
M.Moman Shahzad	BE-CE-2009-85
Hamid Ali Khan	BE-CE-2009-35

PROJECT ADVISOR:

Dr. Kamran Akhtar

HOD
DEPARTMENT OF GEO-TECHNICAL ENGINEERING
NICE
NATIONAL UNIVERSITY OF SCIENCES AND TECHNOLOGY (NUST)

Certificate

This is to certify that work in this thesis has been carried out by **Mr. Waleed Hasan, Mr. Muhammad Moman Shahzad, Mr. Abu Bakr Jamil, Mr. Jawad Mughal** and **Mr. Hamid Ali Khan,** completed under my supervision, NUST Institute of Civil Engineering, School of Civil and Environmental Engineering, National University of Sciences and Technology, H-12, Islamabad, Pakistan.

Project Advisor: **Dr Kamran Akhtar**

Department of Geo-Technical Engineering ,
NUST Institute of Civil Engineering,
School of Civil and Environmental Engineering,
National University of Sciences and Technology,
Islamabad

Submitted through:

_____

Project Advisor: **Dr Kamran Akhtar**

Department of Geo-Technical Engineering ,
NUST Institute of Civil Engineering,
School of Civil and Environmental Engineering,
National University of Sciences and Technology,
Islamabad

_____

HoD: **Dr Kamran Akhtar**

Department of Geo-Technical Engineering ,
NUST Institute of Civil Engineering,
School of Civil and Environmental Engineering,
National University of Sciences and Technology,
Islamabad

DEDICATION

This final year report is lovingly dedicated to our respective parents who have been our constant source of inspiration. They have given us the drive and discipline to tackle any task with enthusiasm and determination. Without their love and support this project would not have been made possible.

ACKNOWLEDGEMENT

We would like to acknowledge and extend our heartfelt gratitude to the following persons who have made the completion of this Final Year Project thesis possible. Our Project Advisor, Dr. Kamran Akhtar, for his great efforts of supervising and leading us, to accomplish this fine work. Dean (SCEE), Dr. S. Muhammad Jamil for his kind helps in data acquisition. Lastly, we offer our regards and blessings to all of those who supported us in any respect during the completion of the final year project thesis.

Table of Contents

LIST OF FIGURES

LIST OF TABLES

ABSTRACT

The project focuses on understanding the phenomenon of soil liquefaction; the factors triggering it, soil behavior during liquefaction and the methods to mitigate liquefaction. Liquefaction occurs when cohesion less saturated soil losses is strength due to excess pore water pressure, and begins to flow when subjected to external loading. The loading is usually cyclic or seismic loading like earthquakes. This phenomenon has inflicted loss of life and property in different countries like Japan and Taiwan, and therefore requires attention of future civil engineers

The report outlines the methods to evaluate liquefaction, namely simplified semi-empirical procedure and shear wave velocity method. Semi-empirical procedure, evaluates a factor of safety against liquefaction by dividing cyclic stress ratio with cyclic resistance ratio. The cyclic stress ratio is the ratio of maximum and minimum stresses induced by an earthquake. The cyclic resistance ratio is the value of cyclic stress that would lead to liquefaction. Shear wave velocity method is a non penetrative technique that uses value of shear wave velocities to evaluate resistance ratio and eventually the factor if safety.

The report also outlines methods to mitigate liquefaction. Different ground improvement techniques have been explained. Lastly, we have designed and assembled a liquefaction tank to physically demonstrate liquefaction. The components and working of the tank are explained in the report below.

CHAPTER 1

INTRODUCTION

1.1 PROJECT BACKGROUND

1.1.1 SOIL LIQUEFACTION:

Soil liquefaction is a phenomenon in which saturated cohesion less soil losses its strength and stiffness under applied loading. Usually it occurs due to seismic loading. After the soil is being liquefied, then it behaves like a liquid and starts to flow. The vibration caused by earthquakes causes a rise in the groundwater pressure that exists in the spaces between the grains of the soil. The probability of liquefaction increases with the increase in the duration of the earthquake. The only strength that resists liquefaction is the friction between the grains of sand, silt or loess and it reduces with the increase in level of pore water pressure due to seismic loading making a viscous liquid i.e. Quikclay.

Quicksand forms when water saturates an area of loose sand and is unable to escape. Hence it creates liquefiable soil that cannot support weight. As quicksand is a heavy and thick liquid that moves slowly and it takes time for the pressure to build-up liquefaction conditions, sand boiling, and associated phenomena may not be noticeable during the quake. In fact, they often do not appear till the shaking has stopped and sometimes not until 10 to 20 minutes later. Conditions of quick sand or sand boiling can continue for hours or even days after the earthquake, sometimes up to a week.

Liquefaction's better definition given by Sladen (1985) describes "liquefaction as a phenomenon in which a soil mass loses a large percentage of its resistance to shear, when subjected to monotonic, cyclic, or shock loading and flows in a manner that resembles a liquid until the shear stresses acting on the mass is as low as the low shear strength. "

1.1.2 SOILS SUCEPTIBLE TO LIQUEFACTION:

To understand the type of soils which are susceptible to liquefaction, there are two broad criteria:

Compositional Criteria

The compositional and state criteria are important for a complete understanding of the liquefaction phenomena.

A uniformly graded soil is more susceptible to soil liquefaction than a well-graded soil because the reduced tendency for volumetric strain of a well-graded soil decreases the amount of excess pore pressure that can develop under undrained conditions.

For experimental purposes, fine clean sand passing 40 no sieve and retained on 200 no. sieve is generally susceptible to liquefaction. Historically, sands were considered to be the only type of soil susceptible to liquefaction, but liquefaction has also been observed in gravel and silt. Strain-softening of fine grained soils can produce effects similar to those of liquefaction. Fine-grained soils are susceptible to this type of behavior if they satisfy the criteria (Wang, 1979) shown in the table below.

- Fraction finer than 0.005 mm<15%
- Liquid Limit, LL < 35%
- Natural water content > 0.9 LL
- Liquidity Index < 0.75

Liquefaction susceptibility also depends on particle shape. Soil deposits with rounded particles, usually found in the types of deposits described in geological criteria, are more susceptible to liquefaction than soils with angular particles.

State Criteria

There are many factors that can be incorporated in the state of soil deposit. Here are some described that are of importance to the liquefaction susceptibility. At constant confining pressure, the liquefaction resistance increases with the relative density, D_r, and, at constant relative density, the liquefaction resistance increases with increasing confining pressure. Various investigations (Castro, 1969; Geotechnical Engineers, Inc.,1982; and Kramer and Seed,1988;) have shown that pre-existing shear static stress in a soil deposit is critical to a soil's susceptibility to static liquefaction. The higher the initial shear stress, the greater is the liquefaction potential and the smaller disturbance is needed to liquefy the soil.

FIG 1 NIGATA, JAPAN: A city falling prey to liquefaction of soil

1.1.3 IMPORTANCE

Seismic events, in general, can cause a number of dangerous ground conditions that can lead to structural damage and failure resulting in loss of life. Severe ground shaking, lateral spreading (such as land sliding and deposit movement/shifting), as well as 'incoherence'. Incoherence is the propagation of a wave in a structure causing foundation or bridge piers to experience movement that is out of sync with the rest of the structure (see bridge failure from 1964 Earthquake in Niigata, Japan, right, and upper deck collapse of Bay Bridge from San Francisco, California 1989, left). Liquefaction may amplify the potential for those conditions and the damage they cause.

Liquefaction is responsible for extreme property damage and loss of life due to a several variations of failure potential. Liquefied ground is no longer stable to withstand the stresses it is subject to from structural foundations or even its own weight, leading to a variety of potential failures. The witnessed effect on structures with their foundations in a liquefied deposit resembles quicksand with a bearing capacity failure occurring beneath the foundations. The building structures will lean and fall; or at times even split open under the under the strains.

Also, dams and retaining walls are common boundaries to many major bodies of water and their adjacent shores. Both rely on the strength and stiffness properties of soil for their stability.

The failure of the soil around them not only can cause the structure itself to weaken, lean, and possibly even fall; but also can result in 'subsurface landslides', during which the supporting soil at the base of the dam or wall loosens and slides out. Dam and retaining wall failure are especially problematic concerns due to the additional potential for flooding.

1.2 OBJECTIVE:

1.2.1 OBJECTIVE OF THE PROJECT:

As mentioned in previous chapters, we are concentrating our main focus towards the phenomena of liquefaction i.e. how it occurs, why it occurs & the means through which it can be countered. For that the main objective of the project is to design and construct a liquefaction tank to be used during geotechnical engineering lectures and laboratory sessions to demonstrate the liquefaction phenomenon fundamental concept.

1.2.2 PLANNING OF THE PROJECT:

The liquefaction demonstration tank is not anything new. In fact, it is a classic in a geotechnical engineering program. This demonstration experiment tends to leave a lasting impression on the students mind. It is easy to find numerous figures and pictures of a basic quicksand model. For example, Holtz and Kovacs (1981) demonstrate a conceptual design diagram of a liquefaction tank. The model consists of two tanks. The water tank is at the bottom and the top tank contains sand. A pump is used to pump the water from the bottom tank into the sand tank, creates the upward flow in the quicksand tank. Flowing through the porous stone layer at the bottom of the sand tank, the upward water pressure is distributed evenly over the entire base of the sand layer, keeping the pore water pressure constant throughout. Number of piezometers is installed directly onto the sand tank at different level, which enables water heads within the quicksand tank during the experiment to be observed and readings to be taken.

From the literature research, there are two existing quicksand models built at other universities, pictures of which are obtained. Essentially, the concept is similar in both tanks. There are two separate containers, one on the top contains sand specimen and a tank with water at the bottom that will be used to fill and drain the sand tank into. Figure 2.1 shows the model at the University of Illinois which is very similar to the diagram in Holtz and Kovacs (1981). The other liquefaction tank shown in Figure 2.2 is built at the Nanyang Technological University, Singapore. Instead of using pump, a standpipe is used to create and control the upwards flows in the sand tank. Also the piezometers in this model are installed on a separated board. Using flexible tubes, they are connected to valves installed at the side of the tank. A dial-gauge used to measure the vertical settlement of the object on top of the sand mass when it liquefies.

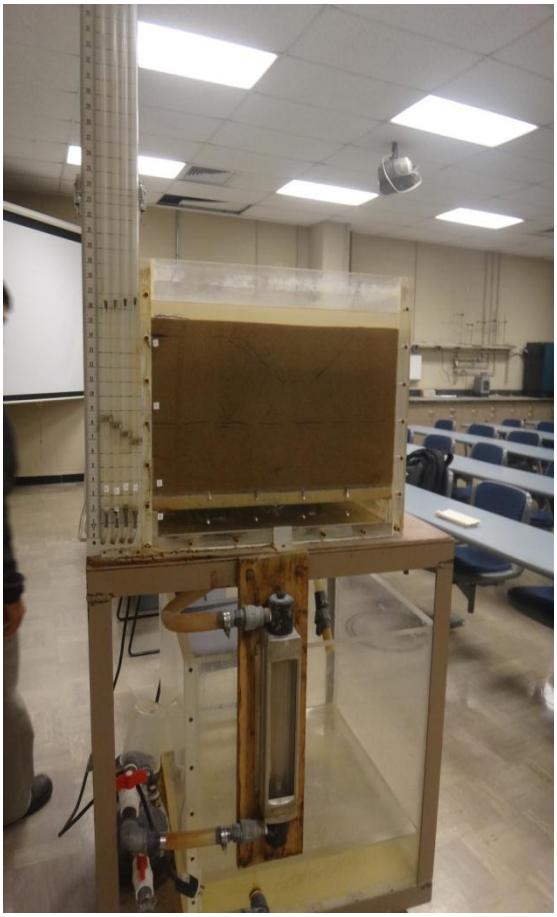

Fig 2.1

Fig 2.2

1.3 LIQUEFACTION OF SATURATED LOOSE SANDS

1.3.1. INTRODUCTION:

Liquefaction is most commonly observed in shallow, loose, saturated cohesion less soils subjected to seismic loading. Unsaturated soils are not subjected to liquefaction because volume compression does not generate excess pore water pressure. Generally loose sand deposits experience raise in pore pressure during shaking especially when sand layer is sandwiched between impermeable layers. Tendency of granular soils to rearrange when sheared causes liquefaction and any factor that resists soil movement will eventually increase the resistance to liquefaction. Increase in depth of soil reduces the probability of liquefaction due to increase in overburden pressure. Therefore over consolidated soils are more resistant to liquefaction because of their stable arrangement of grains. The liquefaction phenomenon has received serious attention since the devastating earthquakes in 1964; the Good Friday earthquake (Mw=9.2) in Alaska, and Niigata earthquake (Mw=7.5) in Japan. Liquefaction induced damage, such as slope failures, bridge and building foundation failures, and flotation of structures were observed in both of these earthquakes. There are several important parameters causing liquefaction which include saturation, relative density, and magnitude of earthquake, ground motion characteristics, effective

overburden pressure and amount of fines. It is the tendency of loose sand to contract during shaking and resultantly increasing the excess pore pressure.

1.3.2. EVENTS CAUSING LIQUEFACTION:

Liquefaction ground failure occurs as the result of an earthquake in areas where the ground is composed more of sand and silt. There are three different factors that need to combine for liquefaction ground failure to occur. The first is that the land must be primarily made up of loose and granular sediment or sand. The second element needed is a high content of moisture or ground water. Either heavy rain or a high water table can provide this. The third element is a severe shaking of the ground due to an earthquake. When all three of these factors combine ground liquefaction failure can occur.

1.3.3 BEHAVIOUR OF SOIL PARTICLES DURING LIQUEFACTION

It is required to recognize the conditions that exist in the soil and deposit before an earthquake to determine liquefaction. Soil is a grouping of many soil particles that stay in touch with many neighboring soil.

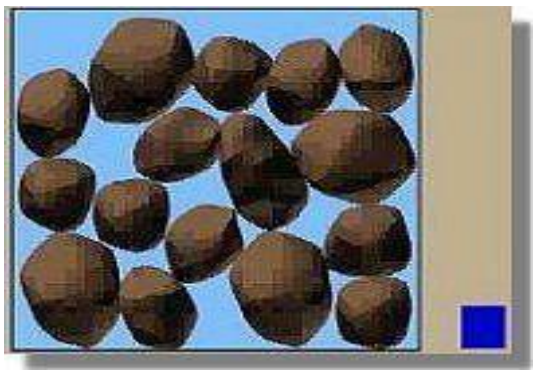

Soil grains in a soil deposit. The height of the blue column to the right represents the level of pore-water pressure in the soil.

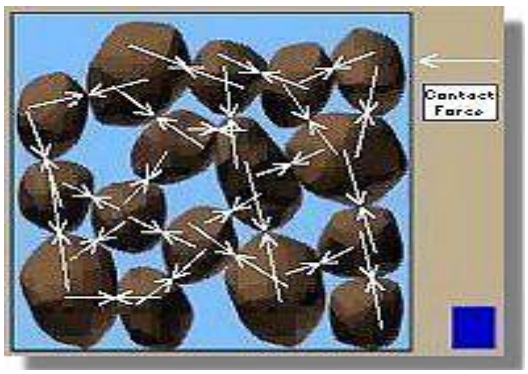

The length of the arrows represents the size of the contact forces between individual soil grains. The contact forces are large when the pore-water pressure is low.

Liquefaction occurs as a result of rapid application of load and breaking of saturated loose sand and loose and packed individual soil particles is trying to move to more densified configuration. However, there is not enough time for the pore water of the soil to be drained out in the case of the earthquake. Instead, water is trapped and prevents soil particles to get close to each other. Thus, there is an increase in water pressure, which reduces the contact forces between soil particles causing softening and weakening the individual soil particles. In extreme conditions, the soil particles may lose contact with each other due to the increased pore water pressure. In such cases, it will have a very low amount of soil strength, and will behave like a liquid rather than a solid material named as liquefaction.

1.4 CASE STUDIES OF LIQUEFACTION:

1.4.1 NIGATA EARTHQUAKE:

Some of the most spectacular examples of settlement and bearing capacity failures due to liquefaction occurred during the Niigata earthquake in 1964. The Niigata earthquake of June 16, 1964, had a magnitude of 7.5 and caused severe damage to many structures in Niigata. The destruction was observed to be largely limited to buildings that were founded on top of loose, saturated soil deposits. Even though numerous houses were totally destroyed, only 28 lives were lost (Johansson 2000).

The Niigata Earthquake resulted in dramatic damage due to liquefaction of the sand deposits in the low-lying areas of Niigata City. In and around this city, the soils consist of recently reclaimed land and young sedimentary deposits having low density and shallow ground water table. At the time of this earthquake, there were approximately 1500 reinforced concrete buildings in Niigata City. About 310 of these buildings were damaged, of which approximately 200 settled or tilted rigidly without appreciable damage to the superstructure. It should be noted that the damaged concrete buildings were built on very shallow foundations or friction piles in loose soil. Similar concrete buildings founded on piles bearing on firm strata at a depth of 20 meters [66 ft] did not suffer damage. Civil engineering structures, which were damaged by the Niigata Earthquake, included port and harbor facilities, water supply systems, railroads, roads, bridges, airport, power facilities, and agricultural facilities. The main reason for these failures was ground failure, particularly due to liquefaction.

Bearing capacity failures: Figure shows dramatic liquefaction-induced bearing capacity failures of Kawagishi-cho apartment buildings located at Niigata, Japan. Figure shows a view of the bottom of

one of the buildings that suffered a bearing capacity failure. Despite the extreme tilting of the buildings, there was remarkably little structural damage because the buildings remained intact during the failure.

● Building settlement: Figures show two more examples of liquefaction induced settlement at Niigata, Japan. Similar to the buildings shown in Figs. and, the buildings remained intact as they settled and tilted. It was reported that there was essentially no interior structural damage and that the doors and windows still functioned. Apparently, the failure took a considerable period of time to develop, which could indicate that the liquefaction started at depth and then slowly progressed toward the ground surface.

● Other damage: It was not just the relatively heavy buildings that suffered liquefaction induced settlement and bearing capacity failures. For example, Fig. shows liquefaction-induced settlement and tilting of relatively light buildings. There was also damage to surface paving materials.

1.4.2 HYOGOKEN NAMBU EARTHQUAKE:

The Kobe earthquake, also known as the Hyogo-ken Nanbu earthquake, had a moment magnitude Mw of 6.9. The earthquake occurred in a region with a complex system of previously mapped active faults. The focus of the earthquake was at a depth of approximately 15 to 20 km (9 to 12 mi). The focal mechanism of the earthquake indicated right-lateral strike-slip faulting on a nearly vertical fault that runs from Awaji Island through the city of Kobe.

Peak ground accelerations as large as 0.8gwere recorded in the near-fault region on alluvial sites in Kobe. In terms of regional tectonics, Kobe is located on the southeastern margin of the Eurasian plate, where the Philippine Sea plate is being sub ducted beneath the Eurasian plate. More than 5000 people perished, more than 26,000 people were injured, and about $200 billion in damage were attributed to this earthquake.

Extensive liquefaction of natural and artificial fill deposits occurred along much of the shoreline on the north side of the Osaka Bay. Probably the most notable were the liquefaction failures of relatively modern fills on the Rokko and Port islands. On the Kobe mainland, evidence of liquefaction extended along the entire length of the waterfront, east and west of Kobe, for a distance of about 20 km [12 mi]. Overall, liquefaction was a principal factor in the extensive damage experienced by the port facilities in the affected region. Most of the liquefied fills were constructed of poorly compacted decomposed granite soil. This material was transported to the fill sites and loosely dumped in water. Compaction was generally only applied to materials placed above water level. As a result, liquefaction occurred within the underwater segments of these poorly compacted fills. Typically, liquefaction led to pervasive eruption of sand boils and, on the islands, to ground settlements on the order of as much as 0.5 m [see Fig. 3]. The ground

settlement caused surprisingly little damage to high- and low-rise buildings, bridges, tanks, and other structures supported on deep foundations. These foundations, including piles and shafts, performed very well in supporting superstructures where ground settlement was the principal effect of liquefaction.

Where liquefaction generated lateral ground displacements, such as near island edges and in other waterfront areas, foundation performance was typically poor. Lateral displacements fractured piles and displaced pile caps, causing structural distress to several bridges. In a few instances, such as the Port Island Ferry Terminal, strong foundations withstood the lateral ground displacement with little damage to the foundation or the superstructure.

There were several factors that apparently contributed to the damage at the Port of Kobe, as follows:

1. **Design criteria**: The area had been previously considered to have a relatively low seismic risk, hence the earthquake design criteria were less stringent than in other areas of Japan.

2. **Earthquake shaking**: There was rupture of the strike-slip fault directly in downtown Kobe. Hence the release of energy along the earthquake fault was close to the port. In addition, the port is located on the shores of a large embayment, which has a substantial thickness of soft and liquefiable sediments. This thick deposit of soft soil caused an amplification of the peak ground acceleration and an increase in the duration of shaking.

3. **Construction of the port**: The area of the port was built almost entirely on fill and reclaimed land. As previously mentioned, the fill and reclaimed land material often consisted of decomposed granite soils that were loosely dumped into the water. The principal factor in the damage at the Port of Kobe was attributed to liquefaction, which caused lateral deformation (also known as lateral spreading) of the retaining walls

4. **Artificial islands**: On Rokko and Port Islands, retaining walls were constructed by using caissons, which consisted of concrete box structures, up to 15 m wide and 20 m deep, with two or more interior cells (Fig. 3). The first step was to prepare the seabed by installing a sand layer. Then the caissons were towed to the site, submerged in position to form the retaining wall, and the interior cells were backfilled with sand. Once in place, the area behind the caission retaining walls was filled in with soil in order to create the artificial islands. During the Kobe earthquake, a large number of these caission retaining walls rotated and slid outward (lateral spreading).. This outward movement of the retaining walls by as much as 3 m (10 ft) caused lateral displacement and failure of the loading dock cranes.

5. **Buildings on deep foundations**: In some cases, the buildings adjacent to the retaining walls had deep foundations consisting of piles or piers. Large differential movement occurred

between the relatively stable buildings having piles or piers and the port retaining walls, which settled and deformed outward.

Fig 3

1.4.3 CHI-CHI EARTHQUAKE:

Numerous liquefaction and sand boiling phenomena were observed in central Taiwan during the 1999 Chi-Chi earthquake. The inland areas suffering the most severe liquefaction damage included Yuanlin, Nantou and Wufeng. The National Center for Research on Earthquake Engineering (NCREE) conducted an extensive investigation in these areas, and many valuable data were obtained. In the Chang–Bin industrial park, which is located in a newly reclaimed land that was created by hydraulic filling, evidences of liquefaction were reported in unimproved sites. However, no sand boil was observed at the improved sites in this industrial park. Figure shows the counties in central west Taiwan that were affected by soil liquefaction in the Chi-Chi earthquake. In particular, the liquefaction manifestations in the towns of Wufeng, Nantou, and Yuanlin, and in the Chang–Bin industrial park are more apparent and more extensive than at

other towns. These areas were the focus of the investigation reported herein. Two hundred and seventy five (275) CPT soundings were collected from these areas, including 28 soundings in Nantou, 13 soundings in Wufeng, 201 soundings in Yuanlin area, 30 soundings in Chang–Bin, and 3 soundings in an adjacent town. The geotechnical characteristics in these areas are derived from the CPT soundings.

Fig 4

1.4.4 DAM FAILURES DUE TO LIQUEFACTION:

A classic example of a flow slide was the failure of the Lower San Fernando Dam caused by the San Fernando earthquake, also known as the Sylmar earthquake. Particulars concerning this earthquake are as follows (Southern California Earthquake Data Center 2000):

● Date of earthquake: February 9, 1971

●Moment magnitude Mw of 6.6

● Depth: 8.4 km

● Type of faulting: Thrust fault

● Faults involved: Primarily the San Fernando fault zone

● Surface rupture: A zone of thrust faulting broke the ground surface in the Sylmar–San Fernando area (northeast of Los Angeles, California). The total surface rupture was roughly 19 km (12 mi) long. The maximum slip was up to 2 m (6 ft).

● Deaths and damage estimate: The earthquake caused more than $500 million in property damage and 65 deaths. Most of the deaths occurred when the Veteran's Administration Hospital collapsed.

● Earthquake response: In response to this earthquake, building codes were strengthened and the Alquist Priolo Special Studies Zone Act was passed in 1972. The purpose of this act is to prohibit the location of most structures for human occupancy across the traces of active faults and to mitigate thereby the hazard of fault rupture.

As mentioned above, the Lower San Fernando Dam was damaged by a flow failure due to the 1971 San Fernando earthquake. Seismographs located on the abutment and on the crest of the dam recorded peak ground accelerations a max of about 0.5 to 0.55g. These high peak ground accelerations caused the liquefaction of a zone of hydraulic sand fill near the base of the upstream shell. Figure 5.1 shows a cross section through the earthen dam and the location of the zone of material that was believed to have liquefied during the earthquake. Once liquefied, the upstream portion of the dam was subjected to a flow slide. The upper part of Fig. 5.1 indicates the portion of the dam and the slip surface along which the flow slide is believed to have initially developed. The lower part of Fig. 5.1 depicts the final condition of the dam after

the flow slide. The flow slide caused the upstream toe of the dam to move about 150 ft (46 m) into the reservoir. Figure 5.2 & 5.3 show two views of the damage to the Lower San Fernando Dam.

A description of the damage is presented below:

General View of the Site

Purpose

In light of the importance of the San Fernando Dam case history and its prominence in the literature, it is important to show how Roc Science, and in particular Phase 2.0, can be used to analyze a case like this.

This example is intended for that purpose. The purpose here is not to replicate all that has been done by others or to necessarily adopt the exact conditions presented by others, but to more generally illustrate the features and capabilities of Roc Science Phase 2.0 in the context of a famous case history.

Fig 5.1 General view of the slide head scarp

Fig 5.2 Upstream face of the dam after drawing down the reservoir

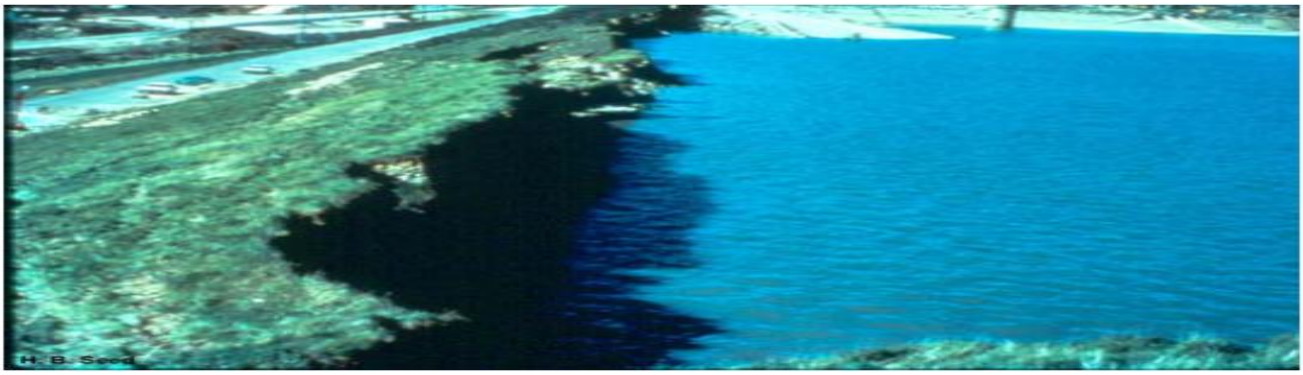

Fig 5.3 A close-up view of the slide head scarp

Phase 2 Result:

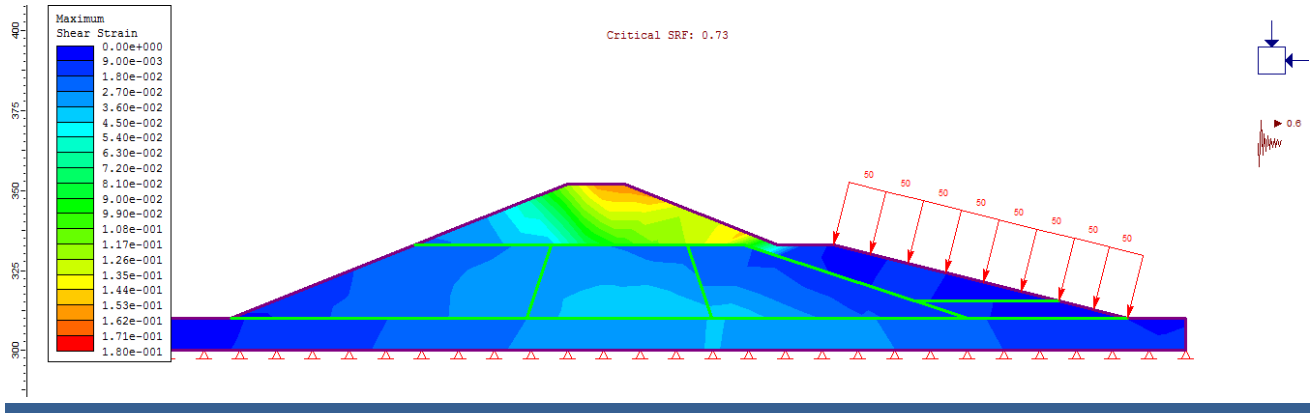

Max. Shear Strain (Undeformed Shape)

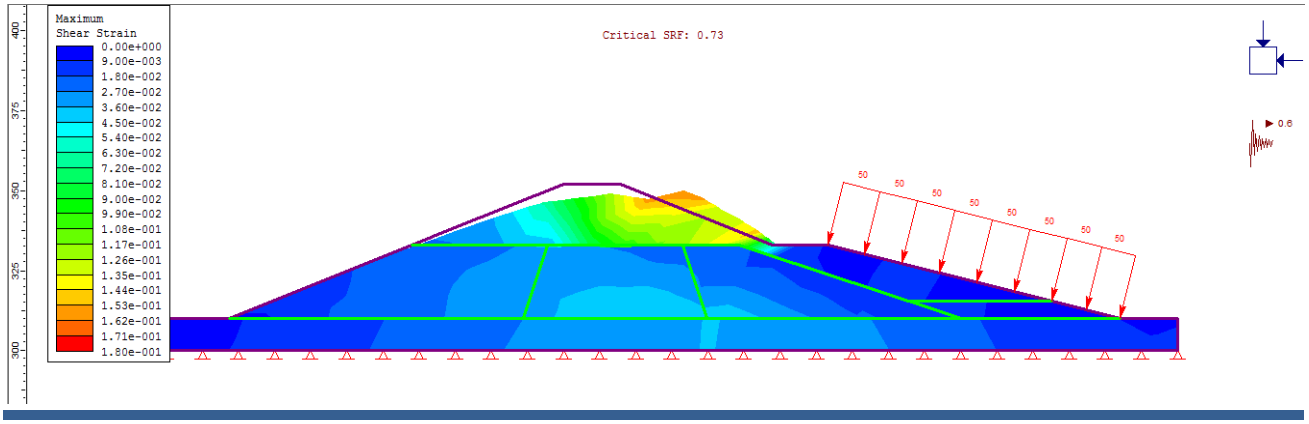

Max. Shear Strain (deformed Shape)

CHAPTER 2

METHODS TO EVALUATE LIQUEFACTION POTENTIAL

2.1 SEMI-EMPIRICAL PROCEDURES FOR EVALUATING LIQUEFACTION POTENTIAL:

Evaluation of the liquefaction potential of saturated cohesionless soils during earthquakes were re-examined and revised using semi-empirical procedures for use in practice by I. M. Idriss, R. W. Boulanger. The stress reduction factor (r_d), earthquake magnitude scaling factor for cyclic stress ratios (MSF*)*, overburden correction factor for cyclic stress ratios (K), and the overburden normalization factor for penetration resistances (CN) were discussed and recently modified relations were presented. These modified relations were used in re-evaluations of the SPT and CPT case history databases. Based on these re-evaluations, revised SPT- and CPT-based liquefaction correlations were recommended for use in practice. In addition, shear wave velocity based procedures and the approaches used to evaluate the cyclic loading behavior of plastic fine-grained soils were also discussed.

Using this procedure, the some SPT and CPT cases of the two major earthquakes, namely Chi-Chi, Taiwan earthquake (magnitude Mw =7.6) and Kocaeli, Turkey earthquake (magnitude Mw = 7.4) in 1999, has been evaluated and compared with the liquefaction potential results obtained from the on-field test for both of them.

Basically, Semi-empirical field-based procedures for evaluating liquefaction potential during earthquakes have two essential components:

(1) The development of an analytical framework to organize past case history experiences.
(2) The development of a suitable in-situ index to represent soil liquefaction characteristics.

There have been a number of re-evaluations to the various components, but the original simplified procedure (Seed and Idriss 1971) for calculating earthquake induced cyclic shear stresses is still the essential component of this analysis framework.

The strength semi-empirical procedure is the use of both experimental findings together with the theoretical considerations for establishing the framework of the analysis procedure. It is far more advanced method of evaluation because it ties together the theory and the field observations.

The paper by I. M. Idriss, R. W. Boulanger provides an update on the semi-empirical field-based procedures for evaluating liquefaction potential of cohesionless soils during earthquakes. This update includes recommended relations for each part of the analytical framework, including the:

- Stress reduction coefficient $\mathbf{r_d}$,
- Magnitude scaling factor **MSF** ,
- Overburden correction factor **K** for cyclic stress ratios, and
- Overburden correction factor **CN** for penetration resistances.

2.1.1 OVERVIEW OF THE FRAMEWORK FOR THE USE OF SEMI-EMPIRICAL LIQUEFACTION PROCEDURES USED IN THIS PAPER:

A brief overview is provided for the framework that is used as the basis for most semi-empirical procedures for evaluating liquefaction potential of cohesionless soils during earthquakes as given by I. M. Idriss, R. W. Boulanger is as follows:

2.1.1.1 The Simplified Procedure for Estimating Cyclic Shear Stress Ratios Induced by Earthquake Ground Motions:

The Seed-Idriss (1971) simplified procedure is used to estimate the cyclic shear stress ratios (***CSR***) induced by earthquake ground motions, at a depth ***z*** below the ground surface, using the following equation (1):

$$CSR = 0.65\left(\frac{\sigma_{vo} a_{max}}{\sigma'_{vo}}\right) r_d \qquad (1)$$

Where a_{max} -maximum horizontal acceleration at the ground surface
σ_o = total vertical stress
σ_o"= effective vertical stress at depth
z = depth
r_d = stress reduction coefficient that accounts for the flexibility of the soil column

2.1.1.2 Adjustment for the Equivalent Number of Stress Cycles in Different Magnitude Earthquakes :

It has been customary to adjust the values of CSR calculated by equation (1) so that the adjusted values of CSR would pertain to the equivalent uniform shear stress induced by the earthquake ground motions generated by an earthquake having a moment magnitude M = 7½, i.e., ($CSR)_{M=7.5}$. Accordingly, the values of $(CSR)_{M=7.5}$are given by equation (2):

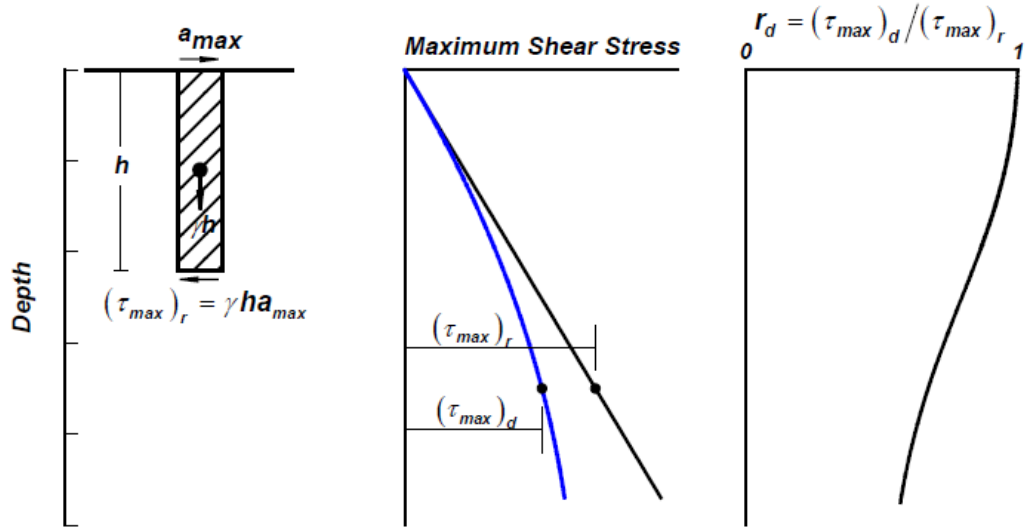

Fig. 1: Schematic for determining maximum shear stress, τ_{max} , and the stress reduction coefficient, r_d .

$$(CSR)_{M-7.5} = \frac{CSR}{MSF} = 0.65\left(\frac{\sigma_{vo} a_{max}}{\sigma'_{vo}}\right)\frac{r_d}{MSF} \qquad (2)$$

Where a_{max} =maximum horizontal acceleration at the ground surface

σ_o =total vertical stress

σ_o"=effective vertical stress at depth

z =Depth

r_d =stress reduction coefficient that accounts for the flexibility of the soil column

MSF= magnitude scaling factor.

2.1.1.3 Use of the SPT Blow Count and CPT Tip Resistance as Indices for Soil Liquefaction Characteristics:

The effective use of SPT blow count and CPT tip resistance as indices for soil liquefaction charactertics require that the effects of soil density and effective confining stress on penetration resistance be separated [Boulanger and Idriss (2004)]. Hence Seed et al (1975a) included the normalization of penetration resistances in sand to an equivalent σ'_{vo} of one atmosphere (1 ***Pa*** =1 tsf =101 kPa) as part of the semi-empirical procedure. This normalization currently takes the form:

$$(N_1)_{60} = C_N (N)_{60} \qquad (3)$$

$$q_{C1} = C_N q_C \qquad (4)$$

2.1.1.4. Stress reduction coefficient, r_d:

The stress reduction coefficient r_d was introduced by Seed and Idriss (1971) as a parameter describing the ratio of cyclic stresses for a flexible soil column to the cyclic stresses for a rigid soil column. They obtained values of r_d for a range of earthquake ground motions and soil profiles having sand in the upper 15± m (50 ft) and suggested an average curve for use as a function of depth. The average curve, which was extended only to a depth of about 12 m (40 ft), was intended for all earthquake magnitudes and for all profiles.

Idriss (1999) extended the work of Golesorkhi (1989) and performed several hundred parametric site response analyses and concluded that for the conditions of most practical interest, the parameter $\mathbf{r_d}$ could be adequately expressed as a function of depth and earthquake magnitude (M**)**. The following relation was derived using those results:

$$Ln(r_d) = \alpha(z) + \beta(z) M$$

$$\alpha(z) = -1.012 - 1.126 \sin\left(\frac{z}{11.73} + 5.133\right)$$

$$\beta(z) = 0.106 + 0.118 \sin\left(\frac{z}{11.28} + 5.142\right)$$

These equations given above were considered for z<=34 m. for z >34 m the equation to be used is:

$$r_d = 0.12 \exp(0.22M)$$

Where, z= depth

M=Magnitude of the earthquake

r_d = stress reduction coefficient

2.1.1.5 Magnitude scaling factor, MSF

The magnitude scaling factor, MSF, has been used to adjust the induced CSR during earthquake magnitude M to an equivalent CSR for an earthquake magnitude, M = 7½. The MSF is thus defined as:

$$MSF = CSR_M / CSR_{M=7.5}$$

The values of MSF are calculated by combining correlations of the number of equivalent uniform cycles versus earthquake magnitude and the laboratory based relations between the cyclic stress ratio required to cause liquefaction and the number of uniform stress cycles.

Idriss (1999) re-evaluated the MSF derivation using results of cyclic tests on high quality samples obtained by frozen sampling techniques. The re-evaluated relation was slightly different from the simplified procedure (Seed et al 1975) . The MSF relation produced by this reevaluation is given by:

$$MSF = 6.9 \exp\left(\frac{-M}{4}\right) - 0.058$$

$$MSF \leq 1.8$$

2.1.1.6 Overburden correction factor, K :

By the studies by Boulanger and Idriss (2004) it is found that overburden stress effects on CRR could be represented in either of two ways:

(1) through the additional normalization of penetration resistances for relative state, thereby producing the quantities $(N_1)_{60}$ and q_{C1}.
(2) through a K factor.

The recommended K curves are expressed as (Boulanger and Idriss 2004):

$$K_\sigma = 1 - C_\sigma \ln\left(\frac{\sigma'_{Vo}}{P_a}\right) \leq 1.0$$

$$C_\sigma = \frac{1}{18.9 - 17.3 D_R} \leq 0.3$$

The correlation between $(N_1)_{60}$, q_{c1N} and D_r are re-evaluated for liquefaction evaluation purpose comes out to be:

$$D_R = \sqrt{\frac{(N_1)_{60}}{46}}$$

$$D_R = 0.478\left(q_{c1N}\right)^{0.264} - 1.063$$

The co-efficient C_σ is expressed in terms of $(N_1)_{60}$, or q_{c1N} :

$$C_\sigma = \frac{1}{18.9 - 2.55\sqrt{(N_1)_{60}}}$$

$$C_\sigma = \frac{1}{37.3 - 8.27\left(q_{c1N}\right)^{0.264}}$$

$(N_1)_{60}$ and q_{c1N} are limited to 37 and 211 respectively in these expressions i.e keeping $C_\sigma \leq 0.3$.

2.1.1.7 Normalization of penetration resistances, CN :

One of the most commonly used expressions for the overburden correction was proposed by Liao and Whitman (1986), viz:

$$C_N = \left(\frac{P_a}{\sigma'_{vo}}\right)^{0.5}$$

But after re-evaluation Boulanger and Idriss (2004) subsequently used the relations given below to obtain the following expressions for determining C_N:

$$C_N = \left(\frac{P_a}{\sigma'_{vo}}\right)^m$$

$$C_N = \left(\frac{P_a}{\sigma'_{vo}}\right)^\alpha \leq 1.7$$

$$\alpha = 0.784 - 0.0768\sqrt{(N_1)_{60}}$$

$$C_N = \left(\frac{P_a}{\sigma'_{vo}}\right)^\beta \leq 1.7$$

$$\alpha = 1.338 - 0.249\left(q_{c1N}\right)^{0.264}$$

2.2 SPT-BASED PROCEDURE FOR EVALUATING LIQUEFACTION POTENTIAL OF COHESIONLESS SOILS:

Semi-empirical procedures for the liquefaction potential analysis was developed using the Standard Penetration Test (SPT) for differentiating between liquefiable and non-liquefiable conditions in the 1964 Niigata earthquake, Japan. In this paper semi-empirical approach is used for differentiating between liquefiable and non-liquefiable conditions for 40 SPT cases the two major earthquakes, namely Chi-Chi, Taiwan earthquake (magnitude M_w =7.6) and Kocaeli, Turkey earthquake (magnitude M_w = 7.4) in 1999. Thus following the semi-empirical approach, the CSR and $(N_1)_{60}$ values were re-calculated using the revised r_d, MSF , K and C_N relations recommended herein.

2.2.1. EVALUATION OF CSR

The K factor is usually applied to the “capacity” side of the analysis during design but it must also be used to convert the CSR [Boulanger and Idriss (2004). It is given as follows:

$$(CSR)_{M-7.5} = 0.65\left(\frac{\sigma_{vo}a_{max}}{\sigma'_{vo}}\right)\frac{r_d}{MSF}\frac{1}{K_\sigma}$$

2.2.2. EVALUATION OF CRR:

For the CRR value, at first the SPT penetration resistance was adjusted by Boulanger and Idriss (2004) to an equivalent clean sand value:

$$(N_1)_{60cs} = (N_1)_{60} + \Delta(N_1)_{60}$$

$$\Delta(N_1)_{60} = exp\left(1.63 + \frac{9.7}{FC} - \left(\frac{15.7}{FC}\right)^2\right)$$

The value of the CRR for a magnitude of earthquake=7.5 and an effective vertical stress of 1 atm can be calculated on the basis of the value of $(N1)_{60cs}$ using the following expression:

$$CRR = exp\left\{\frac{(N_1)_{60cs}}{14.1} + \left(\frac{(N_1)_{60cs}}{126}\right)^2 - \left(\frac{(N_1)_{60cs}}{23.6}\right)^3 + \left(\frac{(N_1)_{60cs}}{25.4}\right)^4 - 2.8\right\}$$

2.2.3 DATA USED:

The data used were the SPT case data from two major earthquakes, namely Chi-Chi, Taiwan earthquake (magnitude Mw =7.6) and Kocaeli, Turkey earthquake (magnitude Mw = 7.4) in 1994 as given by Adel M. Hanna, Derin Ural, Gokhan Saygili, "Neural network model for liquefaction potential in soil deposits using Turkey and Taiwan earthquake data", Soil Dynamics and Earthquake Engineering 27 (2007) 521–540. 40 numbers of data were analyzed using semi-empirical procedures for evaluating the liquefaction potential.

2.2.4 CALCULATION AND TABLE:

The following three tables gives the calculation for the values of CSR and CRR, followed by the assessment of liquefaction potential from these values found out by the semi-empirical method.

Table 1: Calculation of CSR by semi-empirical method using SPT case data:

SL.NO	Z	r_d	MSF	$(N_1)_{60}$	$C_{\square}$	σ'_{vo}/Pa	K	σ'_{vo}/σ_{vo}	CSR
1	1	0.779	1.027	6	0.079	0.139	1.156	1.164	0.199
2	1.8	0.778	1.027	8	0.086	0.204	1.137	1.5	0.26
3	2.6	0.777	1.027	7	0.082	0.27	1.107	1.67	0.297
4	3.4	0.778	1.027	5	0.076	0.337	1.083	1.774	0.319
5	4.2	0.777	1.027	5	0.076	0.411	1.068	1.827	0.332
6	5	0.778	1.027	3	0.069	0.473	1.052	1.885	0.349
7	6	0.777	1.027	3	0.069	0.553	1.041	1.936	0.361
8	7	0.777	1.027	19	0.128	0.65	1.055	1.95	0.359
9	8	0.776	1.027	26	0.17	0.745	1.05	1.96	0.362
10	9	0.776	1.027	48	0.811	0.842	1.139	1.968	0.335
11	1	0.779	1.027	3	0.069	0.156	1.128	1.139	.0197
12	1.8	0.778	1.027	5	0.076	0.224	1.114	1.451	0.253
13	3.4	0.778	1.027	2	0.065	0.358	1.067	1.724	0.314
14	4.2	0.777	1.027	10	0.092	0.428	1.078	1.792	0.323
15	6	0.777	1.027	4	0.072	0.567	1.041	1.911	0.357
16	7	0.777	1.027	11	0.096	0.654	1.041	1.941	0.362
17	8.5	0.776	1.027	39	0.336	0.782	1.083	1.977	0.354
18	10	0.777	1.027	25	0.163	0.935	1.011	1.977	0.38
19	1.8	0.778	1.027	7	0.082	0.192	1.135	1.562	0.268
20	2.8	0.778	1.027	4	0.072	0.276	1.093	1.749	0.310
21	3.7	0.777	1.027	6	0.079	0.357	1.081	1.828	0.328
22	5.6	0.777	1.027	5	0.076	0.505	1.052	1.959	0.362
23	6.5	0.777	1.027	17	0.119	0.585	1.064	1.98	0.361
24	8.5	0.776	1.027	49	0.952	0.784	1.232	1.984	0.312
25	4.1	0.777	1.027	7	0.082	0.409	1.073	1.794	0.325
26	5	0.778	1.027	3	0.069	0.482	1.05	1.858	0.344
27	6.6	0.777	1.027	18	0.124	0.616	1.06	1.932	0.354
28	8	0.777	1.027	32	0.223	0.753	1.063	1.943	0.355
29	9.5	0.776	1.027	75	0.314	0.916	0.97	1.938	0.388
30	11	0.776	1.027	33	0.235	1.082	0.98	1.931	0.382
31	12.5	0.775	1.027	33	0.235	1.25	0.948	1.924	0.393
32	15	0.775	1.027	10	0,092	1.464	0.965	1.959	0.393
33	1.6	0.777	1.027	3	0.069	0.249	1.096	1.008	0.179
34	2.6	0.778	1.027	3	0.069	0.423	1.059	1.007	0.185
35	3.5	0.777	1.027	10	0.092	0.541	1.057	1.073	0.197
36	4.2	0.777	1.027	12	0.099	0.607	1.049	1.179	0.218
37	5	0.778	1.027	31	0.213	0.696	1.077	1.27	0.229
38	6.2	0.777	1.027	33	0.235	0.846	1.039	1.363	0.255
39	8	0.777	1.027	31	0.213	1.05	0.99	1.461	0.287
40	10.5	0.776	1.027	8	0.086	1.27	0.98	1.577	0.312

Table 2: Calculation of CRR by semi-empirical method using SPT case data

Sl.no.	FC	$\Delta(N_1)_{60}$	$(N_1)_{60}$	$(N_1)_{60CS}$	CRR
1	90	5.51	6	11.51	0.129
2	94	5.5	8	13.5	0.144
3	100	5.49	7	13.49	0.136
4	87	5.52	5	10.52	0.122
5	74	5.56	5	10.56	0.122
6	92	5.51	3	8.51	0.108
7	97	5.49	3	8.49	0.108
8	70	5.57	19	24.57	0.28
9	58	5.61	26	31.61	0.607
10	5	.0019	48	48.0019	162.26
11	74	5.56	3	5.56	0.108
12	86	5.53	5	1.053	0.122
13	85	5.53	2	7.53	0.102
14	93	5.51	10	15.51	0.16
15	99	5.49	4	9.49	0.115
16	85	5.53	11	16.53	0.17
17	8	0.365	39	390365	3.38
18	6	0.0273	25	25.0273	0.29
19	99	5.49	7	13.49	0.136
20	99	5.49	4	9049	0.115
21	79	5.55	6	11.55	0.129
22	96	5.5	5	10.5	0.122
23	88	5.52	17	22.52	0.24
24	9	0.715	79	49.715	499.25
25	97	5.49	7	12.49	0.136
26	98	5.49	3	8.49	0.108
27	92	5.51	18	23.51	0.25
28	66	5.59	32	37.59	2.036
29	8	0.365	75	75.365	$6*10^{20}$
30	10	1.145	33	34.145	0.935
31	7	0.133	33	33.133	0.93
32	100	5.49	10	15.49	0.16
33	96	5.5	3	8.5	0.108
34	82	5.54	3	8.54	0.108
35	21	4.63	10	14.63	0.153
36	14	2.9	12	14.9	0.153
37	29	5.32	31	36.32	1.48
38	5	0.0019	33	33.0019	0.759
39	5	0.0019	31	31.0019	0.607
40	100	5.49	8	13.49	0.144

2.3. CPT-BASED PROCEDURE FOR EVALUATING LIQUEFACTION POTENTIAL OF COHESIONLESS SOILS

Seed and Idriss (1981) as well as Douglas et al (1981) proposed the use of correlations between the SPT and CPT to convert the then available SPT-based charts for use with the CPT. The CPT-based liquefaction correlation was re-evaluated by Idriss and Boulanger (2003) using case history data compiled by Shibata and Teparaksa (1988), Kayen et al (1992), Boulanger et al (1995, 1997), Stark and Olson (1995), Suzuki et al (1997) and Moss (2003).

The re-evaluation of CPT cases will include the same adjustments and perimeter revisions as in case of SPT re-evaluation. The CSR adjustment remains same as in case of the SPT cases but the CRR –q_{C1N} will be adjusted according to the different values of tip resistance (q_C).

2.3.1. EVALUATION OF CSR

The K factor is usually applied to the "capacity" side of the analysis during design but it must also be used to convert the CSR as given by Boulanger and Idriss (2004). It is given as follows:

$$(CSR)_{M=7.5} = 0.65\left(\frac{\sigma_{vo}\, a_{max}}{\sigma'_{vo}}\right)\frac{r_d}{MSF}\frac{1}{K_\sigma}$$

2.3.2. EVALUATION OF CRR

The revised CRR – qC1N relation, derived using the considerations can be expressed as follows:

$$CRR = exp\left\{\begin{array}{l}\frac{q_{c1N}}{540}+\left(\frac{q_{c1N}}{67}\right)^2 \\ -\left(\frac{q_{c1N}}{80}\right)^3+\left(\frac{q_{c1N}}{114}\right)^4-3\end{array}\right\}$$

Where,

$$q_{C1} = C_N q_C$$

2.3.3. DATA USED, CALCULATION AND TABLE

The datas used were the CPT case datas from two major earthquakes, namely Chi-Chi, Taiwan earthquake (magnitude Mw =7.6) and Kocaeli, Turkey earthquake (magnitude Mw = 7.4) in 1994 as given by Adel M. Hanna, Derin Ural, Gokhan Saygili, "Evaluation of liquefaction potential of soil deposits using artificial neural networks". 28 numbers of data were analyzed using semi-empirical procedures for evaluating the liquefaction potential.

The following three table gives the calculation for the values of CSR and CRR, followed by the assessment of liquefaction potential from these values found out by the semi-empirical method.

Table 3: calculation of CSR by semi-empirical method using CPT case data

Sl.no.	Z	r_d	MSF	$\frac{\sigma_{vo}}{}$	CSR
1	3.6	0.78	1.027	1.76	0.348
2	4.8	0.78	1.027	1.97	0.389
3	5.8	0.78	1.027	1.65	0.326
4	3.6	0.796	0.97	1.42	0.136
5	17.8	0.793	0.97	1.82	0.174
6	7	0.796	0.97	1.75	0.355
7	3.2	0.797	0.97	1	0.203
8	9.6	0.795	0.97	1.82	0.651
9	8.6	0.795	0.97	1.81	0.646
10	4.4	0.778	1.027	1.81	0.357
11	3.6	0.777	1.027	1.09	0.214
12	11	0.776	1.027	1.89	0.371
13	9.8	0.795	0.97	2.01	0.428
14	11.6	0.795	0.97	1.15	0.11
15	7.8	0.795	0.97	1.8	0.173
16	15.8	0.793	0.97	1.87	0.378
17	3.4	0.797	0.97	1.77	0.359
18	9.8	0.776	0.97	1.48	0.516
19	4	0.778	1.027	1.78	0.587
20	8.8	0.777	1.027	1.97	0.388
21	12.8	0.794	1.027	1.65	0.332
22	12.6	0.794	0.97	1.74	0.167
23	6	0.796	0.97	1.87	0.18
24	2.6	0.796	0.97	1.0	0.203
25	7	0.795	0.97	1.63	0.33
26	2.6	0.796	0.97	1.57	0.561
27	5.2	0.796	0.97	1.8	0.643
28	8.6	0.795	0.97	1.64	0.585

Table 4: Calculation of CRR using CPT based data

Sl.no	C_N	q_{C1}	q_{C1N}	CRR
1	1.63	941.33	9.32	0.052
2	1.27	1533.53	15.18	0.054
3	1.37	1013.66	10.04	0.0517
4	1.54	2808.96	27.8	0.0599
5	0.74	1030.45	10.2	0.0518
6	1.16	2195.53	21.74	0.0565
7	1.4	1400.42	13.87	0.0531
8	1	5285.3	52.33	0.0798
9	1.02	4831.33	47.8	0.0754
10	1.5	2283.75	22.6	0.0569
11	1.32	6836.68	67.69	0.0968
12	0.96	9525.6	94.3	0.133
13	1.08	4469.5	44.25	0.0722
14	0.9	2797.83	27.7	0.0599
15	1.21	2230.88	22.088	0.0567
16	0.61	2506.49	24.82	0.0582
17	2.72	5254.77	52.03	0.0795
18	0.79	5322.39	52.7	0.08
19	2.46	5940.9	58.82	0.0866
20	1.22	2971.92	29.42	0.061
21	0.68	1832.87	18.15	0.0548
22	0.75	735.53	7.28	0.051
23	1.69	4375.41	43.32	0.0714
24	2.42	4271.78	42.29	0.0705
25	1.17	8063.87	79.84	0.1124
26	3.18	2993.65	29.64	0.061
27	1.75	3706.89	36.7	0.066
28	0.92	3329.2	32.96	0.0633

2.4 SHEAR WAVE VELOCITY METHOD:

2.4.1 INTRODUCTION:

Shear wave velocity method is used in earthquake and geotechnical engineering on a large scale. For the study of resistance of soils to liquefaction this particular method has been brought into attention as an alternative or a supplement to the penetration based procedures according to its advantages

Some study of the in-situ tests on soils has shown that the value of shear wave velocity that is measured by cross-hole tests, down-hole tests, SCPT and SASW test are very much similar to one another to a depth of 5-8 m. So on whole the values obtained by shear wave velocity method are more acceptable/precise than that of SPT tests. The suitability of the evaluations is mainly due to the physical foundation that many factors such as:

- Relative density
- Soil fabric
- Prior earthquake strains affect the liquefaction resistance and shear wave velocity in the same manner

The existence in sands of a threshold shear strain, of the order of 10-2 % makes it suitable to be evaluated for soils liquefaction susceptibility by shear wave velocity method. So for many years since numerous studies have been performed to obtain the correlation between shear wave velocity and liquefaction potential of soils or sands. Following are some of the ways by which this correlation can be established:

1. Methods which are based on combinations of in situ measurements by shear wave velocity and laboratory liquefaction tests. The main purpose of this study was to lay down the fact that soils of same type, which have the same shear wave velocity under the same stress conditions, may have the same liquefaction resistance.
2. Methods which are based on in-situ measurements of shear wave velocity and developing an appropriate relationship between the liquefaction resistance and shear wave velocity. There are some field measurements that support the feasibility of this method.
3. There are also some methods that support penetration-Vs correlation.

The procedure adopted to evaluate liquefaction potential using shear wave velocity method follows the Seed-Idriss simplified procedure based on SPT blow counts. Over the years the

procedure has been found to be reasonably reliable; it has correctly predicted moderate to high liquefaction potential for over 95% of case histories.

During the past decade various simplified procedures for evaluating liquefaction resistance based on Vs have been proposed like Dorby 1981, Seed 1983 and Stokoe 1984. Some of these methods follow the general format of Seed-Idriss simplified procedure, where Vs is corrected to a reference over burden stress and correlated with cyclic stress ratio. Nearly all method were developed with limited or no performance data. In our report we have analyzed the procedure proposed by Andrus and Stokoe in 1999.

The shear wave velocity technique is superior to the other in situ type penetration tests because

(a) the existence of large particles in the soil column (e.g., gravelly soils) likely to disable the performance of penetration tests has little effect on the SWV technique,

(b) It is a non-destructive test,

(c) It is one of the few dynamic soil properties that can be measured both in the laboratory and in the field.

2.4.2 STRESS CORELATED SHEAR WAVE VELOCITY

Following the traditional procedure for correcting the SPT-blow count to account for over burden stress one can also correct V_S to a reference over burden stress

$$V_{S1} = V_S \left(\frac{P_a}{\sigma'_v} \right)^{0.25} \qquad \sigma'_v$$

σ'_v = overburden effective stress

Where V_{S1} is the over burden stress corrected shear wave velocity, Pa is the reference stress which is equal to 100kPa or atmospheric pressure. In using the above equation it is implicitly assumed the initial effective horizontal stress is a constant factor of the effective overburden stress. In sites where liquefaction has occurred the factor Ka is usually assumed to be 0.5.

Another assumption in applying the above equation is that Vs is measured with both the directions of particle motion and wave propagation polarized along principal stress directions and one of these directions is vertical.

2.4.3 CYCLIC RESISTANCE RATIO (CRR)

Since CRR is that limiting value of cyclic stress ratio that will cause liquefaction to occur, we shall evaluate a value of CRR using shear wave velocity and use it to calculate a factor of safety. Andrus and Stokoe proposed the following relationship between CRR and V_{S1}

$$\mathrm{CRR} = \left\{ a \left(\frac{V_{s1}}{100} \right)^2 + b \left(\frac{1}{V_{s1}^* - V_{s1}} - \frac{1}{V_{s1}^*} \right) \right\} \mathrm{MSF}$$

V_{S1}* is the limiting upper value of V_{S1} for liquefaction occurrence and is obtained by V_{S1}*=215-(F.C-5), ‘a’ and ‘b’ are curve fitting factors which are assumed to be 0.022 and 2.8 respectively in our analysis later. They are obtained from the equation of the best fit curve obtained by plotting values of Vs and CSR.

2.4.4 FACTOR OF SAFETY AGAINST LIQUEFACTON

The factor of safety of safety is evaluated by dividing the CSR value with the CRR value obtained from the formula above:

$$FS = \frac{CRR}{CSR}$$

2.4.5 RELATIONSHIP BETWEEN SHEAR WAVE VELOCITY AND SPT BLOW COUNTS

The field data of SPT and SWV collected from the alluvial silty sand deposits was evaluated to seek a correlation between the SWV and SPT. The correlation between SWV and SPT was plotted in Fig. 5. This is based on the research by Kamil Kayabah in University of Ankara, Department of Geological Engineering, Tandogan, Turkey.

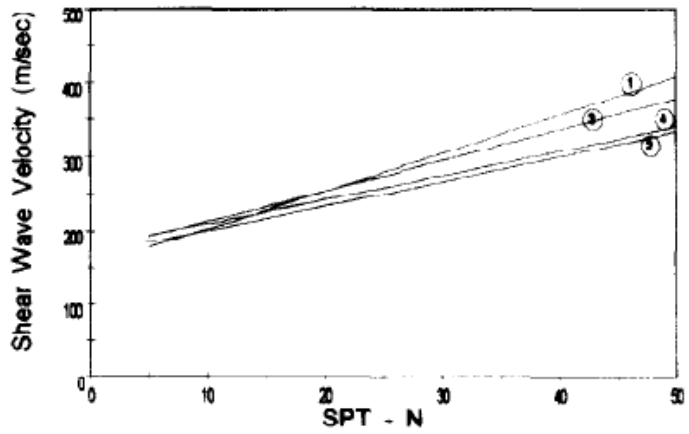

$$V_s = 175 + 3.75N_{60}.$$

Since we do not have the apparatus to evaluate shear wave velocity values from the site, we converted the N_{60} values we had to V_{s1} and formed an excel spread sheet that shows the value of FS against liquefaction using shear wave velocity method

Table 5: Calculation using shear wave velocity

Depth (m)	ϒ	N60	Effective Stress s'vo	Vs	Vs1	FC	Vs1ˆ	CRR	CSR	FOS	Remarks
0.00	17.00	0.00	0.00	175	N/A	7.00	214	N/A			
1.00	18.50	33.60	18.50	301	460.4716	7.00	214	0.504964	0.1	5.04964	SAFE
2.00	18.50	22.21	37.00	258.2707	332.2416	0.00	215	0.235261	0.1	2.352607	SAFE
3.00	18.50	10.25	55.50	213.4293	248.0905	0.00	215	0.043145	0.1	0.431448	FAIL
4.00	18.50	5.46	74.00	195.4804	211.4583	0.00	215	1.000636	0.9	1.111818	SAFE
5.00	18.50	6.92	92.50	200.9509	205.5814	1.00	215	0.43095	0.9	0.478833	FAIL
6.00	18.50	8.70	111.00	207.6083	202.9286	2.00	215	0.353595	0.9	0.392883	FAIL
7.00	19.00	6.72	133.00	200.1897	187.0287	3.00	215	0.187389	0.9	0.20821	FAIL
8.00	19.00	6.94	152.00	201.0193	181.6378	4.00	215	0.163916	0.9	0.182129	FAIL
9.00	19.00	6.06	171.00	197.7389	173.4892	5.00	215	0.137822	0.9	0.153136	FAIL
10.00	19.00	17.96	190.00	242.358	207.1087	6.00	214.5	0.525646	0.8	0.657057	FAIL
11.00	19.00	15.25	209.00	232.1917	193.749	7.00	214	0.237346	0.8	0.296682	FAIL
12.00	19.00	21.17	110.28	254.3874	249.0581	8.00	213.5	0.050958	0.17	0.299751	FAIL
13.00	19.50	19.29	125.97	247.3342	234.2322	9.00	213	-0.02778	0.16	-0.17363	FAIL
14.00	19.50	16.77	135.66	237.8987	221.161	10.00	212.5	-0.26144	0.16	-1.63402	FAIL
15.00	19.50	15.04	145.35	231.4073	211.4475	11.00	212	5.886695	0.15	39.24463	SAFE
16.00	19.50	13.41	155.04	225.3034	202.5751	12.00	211.5	0.446408	0.15	2.976053	SAFE
17.00	19.50	9.50	164.73	210.6311	186.5343	13.00	211	0.203028	0.15	1.353519	SAFE
18.00	19.50	9.84	174.42	211.9048	184.9997	14.00	210.5	0.196255	0.14	1.40182	SAFE
19.00	19.50	12.99	184.11	223.7078	192.682	15.00	210	0.262775	0.14	1.876967	SAFE
20.00	19.50	11.25	193.80	217.1849	184.6803	16.00	209.5	0.199325	0.14	1.423751	SAFE
21.00	19.50	9.88	203.49	212.0514	178.1291	17.00	209	0.168053	0.13	1.292718	SAFE
22.00	19.50	12.33	213.18	221.255	183.7113	18.00	208.5	0.198516	0.13	1.527045	SAFE
23.00	19.50	13.64	222.87	226.1389	185.6914	19.00	208	0.214663	0.13	1.651251	SAFE
24.00	19.50	20.54	232.56	252.0188	204.7521	20.00	207.5	1.253994	0.13	9.646107	SAFE
25.00	19.50	21.13	242.25	254.2358	204.4561	21.00	207	1.346985	0.12	11.22487	SAFE
26.00	19.50	19.73	251.94	248.9972	198.2894	22.00	206.5	0.472903	0.12	3.940859	SAFE

27.00	19.50	18.40	261.63	243.9833	192.472	23.00	206	0.314022	0.12	2.616849	SAFE
28.00	19.50	14.26	271.32	228.4791	178.6099	24.00	205.5	0.183563	0.12	1.529688	SAFE
29.00	19.50	19.62	281.01	248.5686	192.6172	25.00	205	0.335955	0.12	2.799625	SAFE
30.00	19.50	19.29	290.70	247.3321	190.0415	26.00	204.5	0.296355	0.12	2.469626	SAFE
31.00	19.50	17.62	300.39	241.0733	183.7203	27.00	204	0.226876	0.11	2.062505	SAFE
32.00	19.50	18.23	310.08	243.3677	184.0025	28.00	203.5	0.233426	0.11	2.122057	SAFE
33.00	19.50	17.52	319.77	240.6818	180.5773	29.00	203	0.208847	0.11	1.898607	SAFE
34.00	19.50	17.26	329.46	239.7087	178.51	30.00	202.5	0.197622	0.35	0.564635	FAIL
35.00	19.50	16.16	339.15	235.5887	174.175	31.00	202	0.175364	0.35	0.501041	FAIL
36.00	19.50	16.77	348.84	237.8855	174.6388	32.00	201.5	0.179857	0.35	0.513876	FAIL
37.00	19.50	12.82	358.53	223.0732	162.6467	33.00	201	0.133971	0.35	0.382773	FAIL
38.00	19.50	9.79	368.22	211.725	153.3468	4.00	215	0.096103	0.35	0.274579	FAIL
39.00	19.50	12.08	377.91	220.3139	158.5346	5.00	215	0.104936	0.35	0.299817	FAIL
40.00	19.50	12.73	387.60	222.7268	159.2597	5.00	215	0.106252	0.35	0.303577	FAIL
41.00	19.50	15.32	397.29	232.4533	165.1916	5.00	215	0.117923	0.35	0.336923	FAIL
42.00	19.50	24.06	406.98	265.2421	187.3607	5.00	215	0.189075	0.35	0.540214	FAIL
43.00	19.50	21.10	416.67	254.1171	178.4495	5.00	215	0.152667	0.35	0.436192	FAIL
44.00	19.50	19.72	426.36	248.9468	173.8168	5.00	215	0.138721	0.35	0.396347	FAIL
45.00	19.50	21.37	436.05	255.1513	177.1508	5.00	215	0.148504	0.35	0.424296	FAIL
46.00	19.50	17.06	445.74	238.9766	165.0115	5.00	215	0.117542	0.35	0.335835	FAIL
47.00	19.50	17.98	455.43	242.4201	166.4917	5.00	215	0.120728	0.35	0.344937	FAIL
48.00	19.50	18.88	465.12	245.7986	167.9258	5.00	215	0.123942	0.35	0.354121	FAIL
49.00	19.50	18.33	474.81	243.7249	165.653	5.00	215	0.118907	0.35	0.339735	FAIL

2.4.5 SUMMARY AND CONCLUSIONS

There was a good agreement between the laboratory test data and the field performance criteria. Recent strong earthquake data further validated the effectiveness and reliability of this laboratory correlation. This demonstrates the possible link between field and laboratory measurements of shear wave velocities. This link creates the opportunity to extend this approach to study other materials, such as silty sands and gravelly soils, and to study the influence of other parameters, such as high confining pressure, where little to no field performance data are available.

Meanwhile, in consideration of the complexity of liquefaction assessment, this laboratory correlation should be used cautiously and with engineering judgment when applying it to sites where conditions are different from those presented here, especially for those sites subjected to stronger seismic motions or with very low shear wave velocities.

The limitations of the SWV technique are:

- The limited field performance data from earthquake areas for establishing a correlation between SWV and soil liquefaction
- SWV soundings are usually performed at large intervals (as large as 1m)
- No soil sample is recovered through the SWV technique.

CHAPTER 3:

METHODS TO MITIGATE LIQUEFACTION

3.1 INDUCED-PARTIAL SATURATION FOR LIQUEFACTION MITIGATION

3.1.1 INTRODUCTION

Liquefaction of loose saturated sands and has been observed in almost all moderate to large earthquake happened. During an earthquake, saturated loose sands may lose shear strength, coupled with a sudden increase in pore water pressure, often resulting in large lateral dispersion, settlement and the foundation and building damage. Over the past three decades, intensive efforts have been made by the community of geotechnical research to understand the mechanism of liquefaction and develop methods for evaluating the liquefaction potential of a site for a given earthquake. Recent research Mitchell et al. 1995 focused on the use of various soil remediation measures to reduce or eliminate the potential for liquefaction. These measures include: Improving the condition of the site through intensification, increased drainage, thus increasing the effective stress strength, and change of soil fabric with grout.

These corrective measures to protect structures against damage induced by liquefaction are expensive and are often applied in projects involving large and important structures. The potential vulnerability of existing structures based on liquefiable soils continues to be a major concern worldwide. Profitable liquefaction mitigation techniques, that can be easily and widely used for the new and, more importantly, for existing structures are urgently needed. The results of research by many researchers have shown a small reduction in the degree of saturation of sand fully saturated may cause a significant increase in shear strength against liquefaction. Martin et al. 1975 explained that a 1% reduction in the rate of saturation of a sample of saturated sand with 40% porosity can lead to a reduction of 28% of the increase in pore water pressure per cycle. According to Yang et al. 2003, a reduction of the saturation of 1% leads to a reduction in the ratio of pore pressure in excess of 0.6 to 0.15 in a pure horizontal excitation. Chaney 1978 and Yoshimi and al.1989 showed that the liquefaction resistance was about twice that of fully saturated when the degree of saturation reduced to 90% samples. Also, Hu Xia and 1991 showed that trace amounts of trapped air can greatly increase the strength of liquefaction of a sand sample. Their laboratory data showed that the reduction in the degree of saturation from 100 to 97.8% resulted in more than 30% increase in the strength of liquefaction.

3.1.2 AIR ENTRAPMENT AS A LIQUEFACTION MITIGATION MEASURE

During liquefaction the pore water pressure becomes high enough to counter the effective vertical stress, such that the vertical effective stress becomes zero.

Recently, certain laboratory tests have shown the impact of partial saturation on pore water pressure (Yang et al, 2003, Ishihara et al 2002). Initial research has shown that partially saturated sand shows greater resistance against liquefaction as compared to saturated sand of the same density (Xia Hu et al 1991, Ishihara et al, 2002, 1978 Shani, Yoshimi others 1989).

Figure 6 shows the concept of entrapment of air/ gas as a liquefaction mitigation measure. Basically, since air entrapment increases compressibility of the pore fluid (water), which is non-compressible, excess pore pressure can be relieved by the low volume of air bubbles. Therefore, low excess pore water pressure increases effective pressure, and thus the resistance of soil to liquefaction

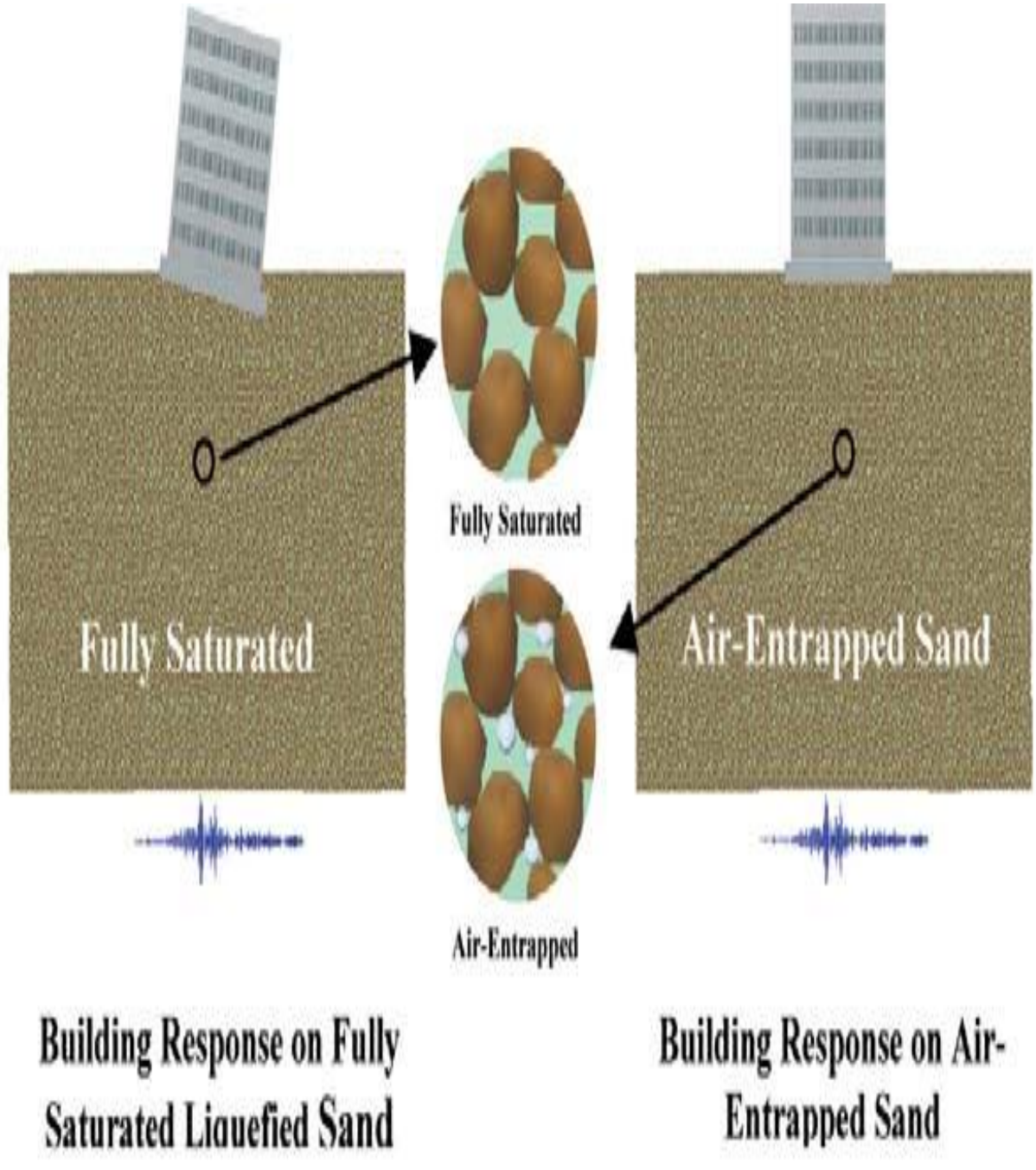

3.2 GROUND IMPROVEMENT TECHNIQUES

3.2.1 CATEGORIES OF GROUND IMPROVEMENT METHODS FOR LIQUEFACTION MITIGATION

Potential Improvement Methods	Principle	Improvement Mechanism
• Compaction grouting • Vibro-systems (vibratory probe, vibro-compaction, vibro-replacement)	Soil particles moved into tighter configuration increasing density	Densification
• Particulate grouting • Chemical grouting • Jet grouting	Soil particles bound together by filling voids with cementing material	Cementation
• Mixed-in-place columns and walls • Jet grouting • Vibro-replacement • Root piles	Soil mass reinforced with stiff elements used to provide additional shear resistance. When elements are overlapped and arranged to form enclosed areas, containment also provided.	Reinforcement and Containment
• Surcharge or buttress2 fill • Compaction grouting1	In-situ effective stresses within soil mass are increased resulting in an increase in shear resistance.	In-situ stress Increase
• Gravel, sand, and wick drains • Vibro-replacement1	High permeability drainage elements installed to decrease drainage distance in soil mass limiting development, and providing faster dissipation, of excess pore water pressures.	Drainage

Table 6

Notes:

1. For this specific treatment method the cited improvement mechanism is generally considered to be a secondary mechanism.
2. When used at the toe of a slope, a buttress fill also provides additional mass to

resist a slope stability failure and increases the potential failure surface length.

3.2.1.1 Compaction Grouting

Compaction grouting involves the injection of a very stiff grout (soil-cement-water mixture with sufficient silt sizes to provide plasticity, together with sand and gravel sizes to develop internal friction) that does not permeate the native soil, but results in controlled growth of the grout bulb mass that displaces the surrounding soil. The primary purpose of compaction grouting is to increase the density of soft, loose or disturbed soil, typically for settlement control, structural re-leveling, increasing the soil's bearing capacity, and mitigation of liquefaction potential.

As shown in Figure (a), compaction grouting involves the installation of casing to the required depth into a pre-drilled hole (70~100mm diameter). The stiff grout is then pumped through the casing at high pressure until typically one of three criteria is reached, i.e.,

- target volume;
- maximum pressure; or surface (sub-surface) heave. The grouting is performed in typically 0.3~0.9m intervals or stages,

(a)

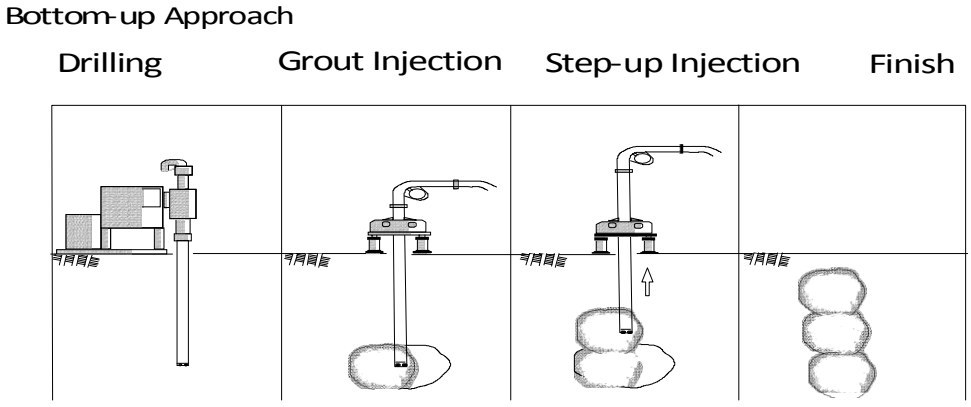

Fig (b)

Fig 7 Compaction grouting implementation; and (b) Grout injection under high pressure

thus forming a column of interconnected grout bulbs. At each stage, the soil particles are displaced radially from a growing bulb of grout through cavity expansion effects into a closer spacing, thus increasing the density of the adjacent soil around the bulb. Note that the strength of the grout is unimportant because the purpose of the technique is to density the surrounding soil by displacement. Compaction grouting can either be performed "top-down," i.e., from the upper to the lower limit of the treatment zone or, more commonly, in a "bottom-up" process from the lower limit upwards. Figure(b) shows a typical process of injecting the grout.

The method was most effective on sandy soil with fewer fines content. In addition, compaction grouting also increased the strength and the lateral earth pressure of the ground

3.2.1.2 VIBRO-COMPACTION

The most commonly used ground improvement technique that result in densification are vibro-compaction, vibroreplacement, dynamic compaction and sand compaction pile. Vibro-compaction provides an economical and effective method to density deep granular non-cohesive deposits. In vibro-compaction, a vibrating probe (or vibroflot) is repeatedly raised and lowered through the soil, inducing local temporary liquefaction. During liquefaction, the inter-granular particle forces become zero, and gravitational forces rearrange the soil particles into a denser unstressed state, permanently strengthening the soil. During the state of temporary liquefaction, material is fed and compacted into the voids created by the liquefaction, creating densified sand columns. Re-liquefaction of the soil can only occur if subsequent dynamic loading is more intense than the vibrations induced by the vibro-compaction process.

OVERVIEW OF THIS TECHNIQUE

The essential equipment for this process is a depth vibrator a long, heavy tube enclosing eccentric weights, driven by an electric motor. The vibrator is connected to a source of electric power and a high-pressure water pump. Extension tubes are added as necessary, depending on the treatment depth, and the whole assemblage is suspended from a crane. With the electric power and water supply switched on, the vibrator is lowered into the ground. The combination of vibration and high pressure water jetting, causes liquefaction of the soils surrounding the vibrator, which assists in the penetration process.

When the required depth is reached, the water pressure is reduced and the vibrator pulled up in short steps. With the inter-particle friction temporarily reduced, the surrounding soil particles then fall back below the vibrator and, subjected to vibratory

energy, are rearranged into a denser state. This process is repeated back up to the ground level, leaving on completion, a column of very dense material surrounded by material of enhanced density. The degree of compaction achieved at a particular point depends on the properties of the soil being treated, the amount of time spent at each compaction step and the distance from the vibrator. The spacing of probes is designed to ensure that the zones of influence overlap sufficiently to achieve minimum requirements throughout the treated area. Generally, the effect of the compaction becomes visible at the ground surface in the form of a cone-shaped depression. The depression formed around the vibrator or the extension tubes is continually in-filled with granular materials, which is either imported or obtained from the natural granular deposits a the site. Water required for the penetration and compaction process is obtained either by direct pumping from nearby water source or ground water using well points. Vibro-compaction is suitable for treating sands with a fines content of less than 10 to 15%. Based on various research work carried out, well established guidelines are available to evaluate where vibration techniques could work successfully. It is generally accepted that the Vibro-replacement works successfully for grain size range from 0.002 to 0.2mm, whereas vibro-compaction could be more appropriate for the grain sizes in the range of 0.2 to 60mm.

Vibro Compaction works were carried out up to a depth of 10m in 3m grid spacings for each area. The crater formed during vibro compaction was filled using the sand available material at site (Fig). For the present area, the consumption of backfill material (sand) was 10 to 14%, which clearly indicates that significant densification has taken place. Also the ground level in compacted area went below by 1m clearly showing the achieving of ground improvement.

Fig.8: Backfilling of Sand as Compensation Material During Vibro Compaction

3.2.1.3 Vibroflotation

Vibroflotation involves the use of a vibrating probe that can penetrate granular soil to depths of over 100 feet. The vibrations of the probe cause the grain structure to collapse thereby densifying the soil surrounding the probe. To treat an area of potentially liquefiable soil, the vibroflot is raised and lowered in a grid pattern. Vibro Replacement (right) is a combination of vibroflotation with a gravel backfill resulting in stone columns, which not only increases the amount of densificton, but provides a degree of reinforcement and a potentially effective means of drainage.

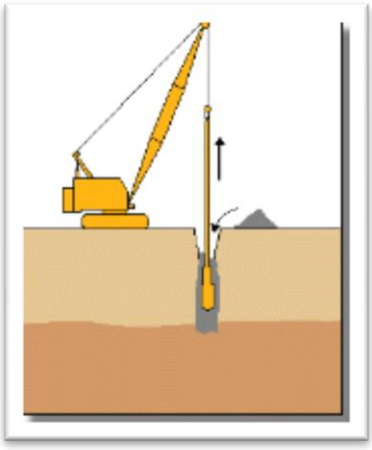

Fig 9: Vibroflotation

3.2.1.4 Dynamic Compaction

Densification by dynamic compaction is performed by dropping a heavy weight of steel or concrete in a grid pattern from heights of 30 to 100 ft. It provides an economical way of improving soil for mitigation of liquefaction hazards. Local liquefaction can be initiated beneath the drop point making it easier for the sand grains to densify. When the excess pore water pressure from the dynamic loading dissipates, additional densification occurs. As illustrated in the photograph, however, the process is somewhat invasive; the surface of the soil may require shallow compaction with possible addition of granular fill following dynamic compaction.

Fig 10

3.2.1.5 Stone Columns

As described above, stone columns are columns of gravel constructed in the ground. Stone columns can be constructed by the vibroflotation method. They can also be installed in other ways, for example, with help of a steel casing and a drop hammer as in the Franki Method(NOTE: The Franki Method is a method used to drive expanded base cast-in-situ concrete (franki) piles. This method can be applied to different site conditions and is still widely used due to its high tensile load capacity, and relatively low noise and ground vibration levels). In this approach the steel casing is driven in to the soil and gravel is filled in from the top and tamped with a drop hammer as the steel casing is successively withdrawn.

3.2.1.6 Compaction Piles

Installing compaction piles are a very effective way of improving soil. Compaction piles are usually made of pre-stressed concrete or timber. Installation of compaction piles both densifies and reinforces the soil. The piles are generally installed in a grid pattern and are generally driven to depth of up to 60 ft.

3.3 Summary of Ground Improvement Methods for Liquefaction Remediation

Method	Principle	Suitable Soil Types	Treated Soil Properties	Relative Costs	Abutment Applicability*		Pier Applicability*	Comments
					Stub	Full-Height Wingwall		
Compaction Grout	Highly viscous grout acts as spherical hydraulic jack when pumped under high pressure resulting in densification.	Compressible soils with some fines	Increased Dr SPT: (N1)60 = 25 to 30 CPT: qc1 = 80 to 150 tsf (Kg/cm2)	Low material cost; high injection cost.	1. High. Treat anywhere between abutment and embankment toe; treat under and around abutment if excessive settlement expected. 2. High. Treat around pile groups.	1. Generally high. Treat under and around foundation. 2. High. Treat around pile groups.	High for solid wall, multi-column, and hammer- head piers. High to moderate for circular column piers. 1. Treat under and around foundation. 2. Treat around pile groups.	Must control heave and/or hydraulic fracture of soil. Particulate and chemi-cal grouting: verify size and strength of grouted soil mass. Jet grouting: stage work to limit settle-ments. Evalu-ate potential damage to piles from jetting pres-sure.
Particulate Grouting	Penetration grouting: fill soil pores with cement, soil and/or clay.	Clean, medium to coarse sand and gravel	Cement grouted soil: high strength	Lowest of grouting systems				
Chemical Grouting	Solutions of two or more chemicals react in soil pores to form a gel or solid precipitate.	Medium silts and coarser	Low to high strength	High to very high				
Jet Grouting	High speed jets at depth excavate, inject and mix	Sands, silts and clays	Solidified columns and walls	High				

	stabilizer with soil to form column or panels.							
Vibratory Probe	Densification by vibration,liquefac-tion-induced settlement underwater.	Sand (< 15% passing No. 200 sieve)	Dr: up to 80+% Ineffective in some sands.	Moderate	1. Moderate for lateral spreading; low for settlement. Treat at embankment toe to reduce risk of con-struction settlement. 2. Low. Treating around piles difficult due to access problems.		1. Low. Potential for excessive settlement and vibrations of bridge. Over-head clearance limitations. 2. Moderate to high. Treat around pile groups.	Overhead clearance limitations will restrict use. Monitor bridge for excessive vibrations. Construction in water requires special procedures.
Vibro-Compaction	Densification by vibration and compaction of backfill at depth.	Sand (<20% passing No. 200 sieve)	Dr: up to 85+% SPT: (N1)60 = 25 to 30 CPT: qc1 = 80 to 150 tsf (Kg/cm2)	Moderate				
Vibro-Replace-ment	Densely compacted gravel columns provide densification, reinforcement, and drainage.	Soft silty or clayey sands, silts, clayey silts	Increased Dr SPT: (N1)60 = 25 to 30 CPT: qc1= 80 to 150 tsf (Kg/cm2)	Moderate to high				
Surcharge/ Buttress Fill	Weight of surcharge increases liquefaction resistance by increasing effective stresses. Buttress fill increases stability by increasing resisting	Any soil surface provided it will be stable	Increase in strength	Low	1. High for slope stability; low for settlement. Place at embankment toe 2. Low. Ineffective in increasing soil stresses at piles.	1 & 2. Mod-erate. Place buttress fill in front of wall.	1 & 2. Moderate to low. Place surcharge around pier.	Need large area. Evaluate loads and settlement imposed on bridge.

	moment and extending failure surface.							
Mix-In-Place Walls & Columns	Lime, cement or asphalt introduced through auger or special in-place mixer.	All soft or loose soils	Solidified soil walls or columns of relatively high strength confine and/or reinforce potentially liquefiable soils	High	1. Moderate for lateral spreading; low for settlement. Install along toe of embankment. 2. Low. Hard to install around abutment pile group.	1. Moderate for lateral spreading, low for settlement. Install at toe of wall. 2. Moderate to low. Install around abut-ment pile group.	1. Moderate to low. Install completely around pier. 2. Moderate to low. Install completely around pier pile groups.	Extend to firm strata. Stage work to control construction settlements. Space limitations may restrict use. Construction in water requires special procedures.
Root Piles	Small-diameterinclusions used to carry tension, shear and compression.	All soils	Reinforcedzone behaves as a coherent mass	Moderateto high	1. Moderatetto low. Zone for installing piles same as described for for grouting.2. Moderatetto low. Install piles around pile groups.	1. Moderate to low. Install piles beneath and around foundation.2. Moderate to low. Install piles aroundpile groups.	1. Moderate tolow. Install piles beneath and around pier founda-tion.2. Moderate to low. Install piles around pile groups.	Extend pilesto firm strata. Largenumber of piles may berequired to provide adequate reinforce - ment. Avoiddamage to existing piles.

Drains: Gravel Sand Wick	Relief of excess porewater pressure to prevent liquefaction. Intercept and dissipate excess pore water pressure plumes from adjacent liquefied soil.	Sand, silt	Improved drainage	Low to moderate	1&2. Mod-erate. Install drains around zone improved by other method(s).	1&2. Moderate .Install drains around zone improved by other method(s) .	1&2. Moderate. Install drains around zone improved by other method(s).	Topography and space limitations may restrict use.

Table 7 Note: *Item no.1 for foundation over or in liquefiable soils. Item no.2 for pile (or drilled shaft) foundations extending through liquefiable soils.

CHAPTER 4:

SAND LIQUEFACTION TANK

4.1 OVERVIEW

Liquefaction is a phenomenon which is difficult to understand if explained theoretically. As students of civil engineering we have learnt that watching civil engineering principles being executed, gives a whole new learning experience; the entire concept becomes clearer and easily comprehensible. Exactly in line with this principle, we thought we should create something that lets students' see for themselves sand liquefaction.

We also felt that in Pakistan there are practically no sites where we can go and asses the liquefaction potential because generally the soil is non-susceptible. After taking up this project we felt that we should try and fill this gap by making a model that is as close as possible to reality and at the same time is compact and fits into the lab premises. This is where we started pursuing the design of liquefaction tank.

The idea is not however something we invented from scratch. But the design of the tank is not available anywhere online. It is available in a few books but not very well explained. So we had to come up with a set of new ideas which when combined with the previous design ideas gives something that works well for our cause.

In our effort we have tried our best to recreate real world scenario. But being students and certain time constraints we haven't been able to accomplish every goal we set out to achieve. We haven't performed any testing using this model, but the model is perfectly capable of being used to test certain mitigation techniques like use of air bubbles.

4.1.1 OBJECTIVE AND IMPORTANCE

The objective behind the creation of the liquefaction tank was to help ourselves understand the behavior of soil particles during liquefaction and the events that trigger the phenomenon. The tank also helps us understand the nature of particles susceptible to liquefaction. We hope that the future generation of students at NUST uses this very model to acquaint themselves with liquefaction.

The tank however is not only limited to just demonstration. The entire apparatus can be used to test the soil potential for liquefaction under different conditions. As outlined in the previous chapter air bubbles can be used to mitigate liquefaction. The preliminary testing of such mitigation measures can also take place in this apparatus. Moreover the see through tank helps us get a step by step update about the state of soil as the water table rises. If a series of photographs is taken or a video is made then, the movement of particles can be analyzed in more detail and innovative methods of mitigation can be proposed.

In countries like Pakistan where there are not many sites that are experiencing liquefaction, it is imperative to use a model to depict this soil behavior. After graduation students sill fly to all parts of the world and work in different capacities and in different countries; so they need to have a good grasp on every civil engineering concept. This liquefaction tank helps tighten a student's grip on one such concept. This model also goes

on to show that liquefaction can be demonstrated in the lab. Most geotechnical problems cannot be recreated in the lab because it is very difficult to replicate the ground conditions in the lab. But as this tank proves, in case of liquefaction a very realistic estimate of real life situation can be made and shown in the laboratory.

4.2 DESIGN

As mentioned earlier we do not take entire credit for the design of the model. But there have been a lot of modifications from the designs we obtained from different sources. These modifications will be explained further in the chapter below.

A lot of components are items of day to day use. Considering are budget constraints we put the most economical set of items together to effectively achieve our objective.

Fig 11 Liquefaction tank

4.2.1 COMPONENT

The sand liquefaction tank is an assembly of different components the purpose, source and design of each is explained below.

4.2.1.1 The iron frame

To hold the entire assembly we needed a strong enough structure. It had to be economical because we wanted to focus most of our financial resources on the tank itself and its working. So we made a 3’ by 3’ by 3’ angle iron frame, which has two storeys and is clearly visible in the picture 4.1.

The stand has wheels beneath all four legs so as to ensure that the model is mobile and can easily be moved within the department premises. The entire iron frame structure and the wheel were designed to bear a load in excess of 1000 kg. According to our estimates weight that was to be placed on the frame was around 550 kg. We still have a healthy margin of safety in terms of weight.

- Weight estimation was as follows
- Sand volume = 2’ x 2 x 2’= 8 cft
- Sand density= 110 lbs/ft3
- Weight of sand= 110 x 8= 880 lbs= 400 kg
- Weight of water (tank inclusive)= 100 kg
- Weight of motor, peizometers etc = 50 kg
- Total= 550 kg

4.2.1.2 The water tank

Fig 12 Water Tank

The water tank used is a regular one hundred liter water tank. In imitating the real world conditions we had to show the effect of the water table. To do so we needed a source of water. We could not connect it directly to a tap because that would make the entire assembly immobile. We could not make a custom made tank because it would become too

expensive. The solution we devised was to buy a tank that is usually used in homes and offices and bring it to use. Our solution proved worthwhile and ever since this tank has been working effectively. The water is drawn from this tank. The outlets and over flow pipes throw water back into this tank, so that there is no wastage of water and we do not have to refill the tank each time we operate it.

The tank is placed on the lower storey of the iron stand as shown in the Figure 1

4.2.1.3 THE ELECTRIC MOTOR

The water had to be pumped from the water tank to the sand tank since the water tank is at a lower height. For this purposes we attached a motor to the tank. The motor has hp and pump upto a head of 20 feet.

The pressure generated by the motor is crucial since this is the pressure which determines the extent of turbulence experienced by the sand particles.

Fig 13 Electric motor to pump the water

4.2.1.4 The inlets to the sand tank

There is a single pipe connecting the water tank and the motor. The pipe going from motor to the sand tank above splits in to four before entering the sand tank. This is done to evenly distribute the pressure from the motor on the sand inside the tank above. The four inlets are controlled by a valve right above the motor. The valve not only starts or stops the supply of water but also controls the pressure of water going into the sand tank. The pipes used in making the four-inlet formation are 0.5 inch diameter iron pipes; iron pipes are used to ensure that the orientation of the four inlets remains permanent and is not disturbed as would have been the case if flexible pipes were used. The pipes extending beyond this four point junction are flexible. This arrangement was economical and reliable.

Figure 14

The four pipes heading towards the sand tank are then attached to four different inlet points at the bottom of the sand tank. The orientation of the inlet pipes in shown in figure 15

Figure 15

The inlets have been effectively sealed with silicon and rubber to avoid any leakages and to maintain the pressure. The inlet holes on the base of the sand tank are 0.5 inch diameter holes.

4.2.1.5 The Porous plate

To recreate the real world conditions we had to ensure that the water rised uniformly in the sand tank, just like a real water table would rise underground. There were two proposals for this: a) To use a porous stone b) To make a porous metal plate. We opted for the latter since it was easily available and cheaper.

The porous metal plate is a 12 gauge metal sheet. That has 0.5 inch holes on it. The holes are in a grid pattern uniformly distributed all over the face of the plate. The sand mass would rest over this plate. To ensure that the sand dose not leak thorough this plate, a 200 no. sieve was fixed on its top face. This would retain the sand and allow the water to pass thorough. To support the plate itself three supports were provided on the base of the tank. The specifications of the supports are given in the next section. The images below show the porous plate and the sieve that was fastened onto its top surface.

Fig 16 Porous metal plate with 200 no sieve on top

Fig 17 200 no. seive

4.2.1.5 The Sand Tank

The most crucial part of the assembly is the sand tank. It had to be transparent so that liquefaction could be seen. At the same time it had to be strong enough to bear internal pressure of sand and water and external forces like a rubber hammer being hit on the tank wall to generate shock waves. Our first proposal was to use 12mm thick glass sheets to make the tank. It was an economical option, the transparency was excellent, the strength was fine and the weight was also within our estimates. But the glass tank was brittle and had to be handled with extreme care. So we went with the only other choice; using a 25mm thick plexi-glass tank. It had all the features a glass tank had to offer except that it was little more expensive, but it had the added advantage of not being brittle.

The specifications of the tank are as follows:

- Length= 2 feet,
- Breadth= 2 feet,
- Height= 2feet,
- Thickness of plexi-glass= 25mm

Since the tank had to be water tight, the surface between any two joints in the tank has been sealed with silicon. All four sides have been held together with screws, to ensure strength. The base of the tank has four 1 inch diameter holes for inlet of water and another two 1 inch diameter holes for outlet of water. There are a total of 6 identical holes in the base. The inlet holes are situated in centre of the base whereas each outlet is

situated at a corner in the base.

Figure 16 shows the sand tank. The four pipes rising from the base of the tank are the

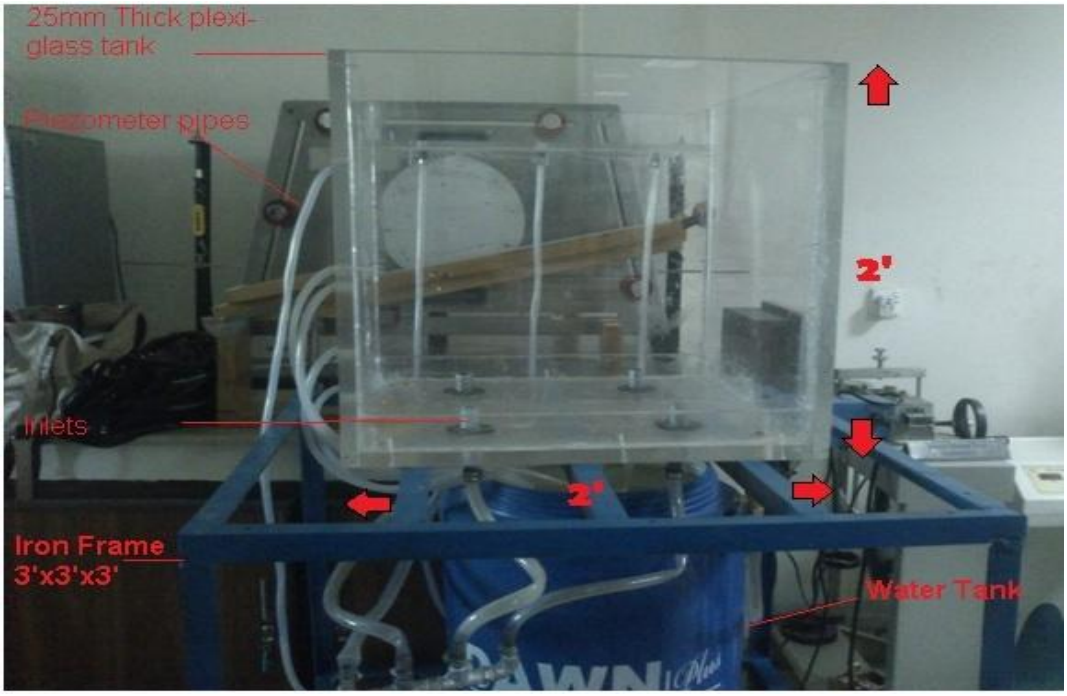

Figure 16 Sand Tank

inlets. Their orientation is such that it ensures uniform inflow of water. The outlets are on diagonally opposite corners of the base and cannot be spotted in the figure above. The outlets are connected to flexible pipes which take the water back into to water tank beneath. Each outlet is fitted with a valve to start and stop the flow of water. One such outlet is shown in the figure 17.

Figure 19 Outlet valve

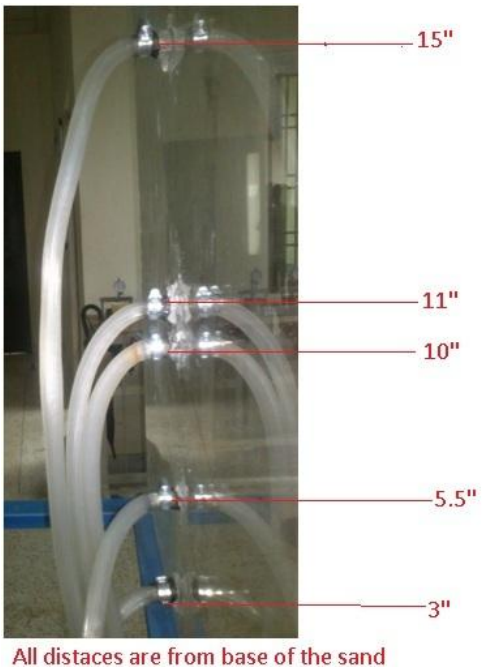

Figure 20 Piezometer pipes

On one face of the sand tank there are five 0.5 inch holes. These holes are the points where the Piezometer pipes are connected. These holes are ata a vertical distance of 3", 5.5", 10", 11" and 15" from the base of the tank.

The piezometers tell us the head of water at different points in the tank and assist us in our analysis of liquefaction. They can be seen in figure 5. The pipes on

Figure 8

your left in figure 5 are the piezometer pipes. A closer view of these pipes can be seen in figure 8.

On a different face of the tank an L section has been provided to act as an overflow channel. The base of the overflow channel has three 0.5 inch diameter holes that provided an escape route to the excess water. These overflow pipes fall back into the water tank beneath and ensure no water is wasted. The overflow pipes are shown in the figure below.

On the inside of the tank there are three 12mm thick supports. These supports are meant to hold the porous plate that would be placed inside the tank. These supports are 6" high, 12mm thick and 22 inches long. Two of the supports are joined with the side wall and one support is in the middle. The supports and the L section are shown in the images below

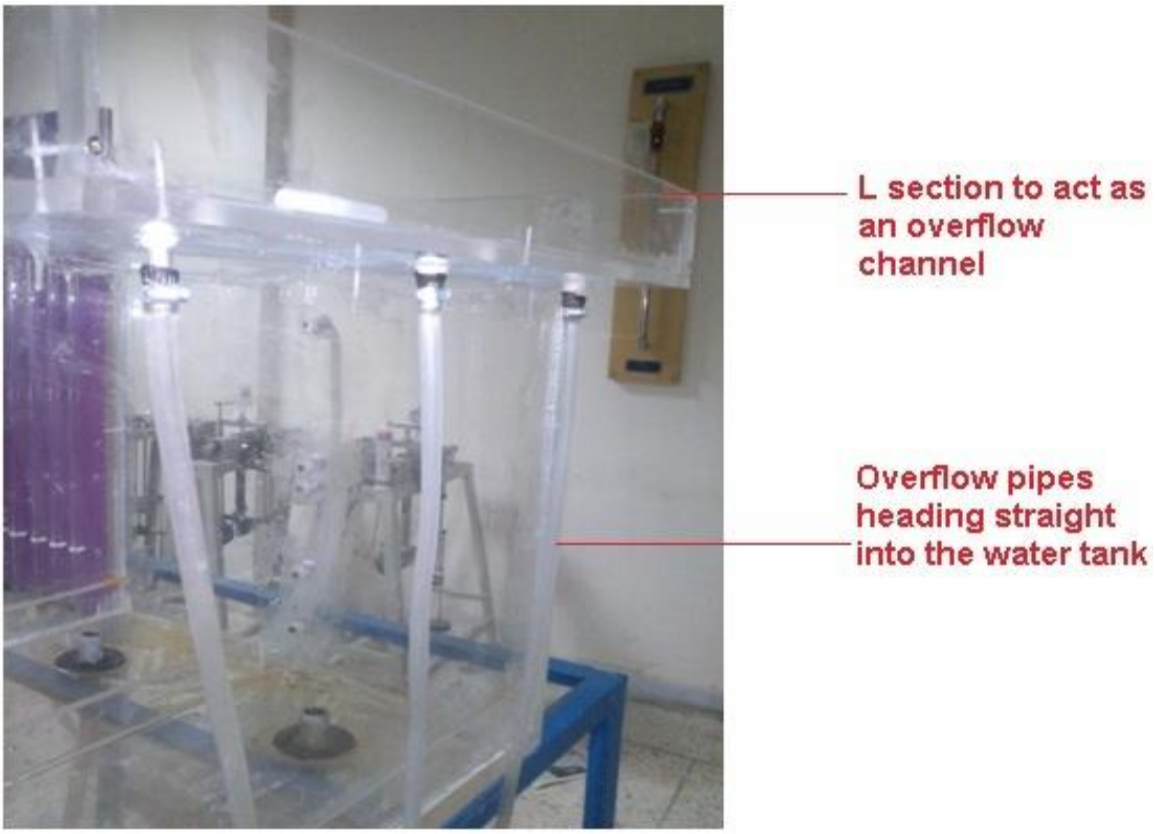

Figure 20 Overflow section

4.2.1.6 Piezometers

The piezometer pipes coming from the sand tank are connected to piezometer tubes. The tubes are mounted on chipboard and the chipboard is fastened onto angle irons to ensure its verticality. The holes in the sand tank for piezometer pipes are covered with 200 no. sieve, so that the sand dose not flow into the piezometer tubes. The water that penetrates that sieves flows through the pipes and rises in the tubes to give head of water.

Fig 21 Piezometers

Knowing the pressure of water at different points is essential, since the behavior of soil for a given pressure head of water can then be seen and analyzed. This helps us determine at what pressure head the soil particles behave in a certain manner.

4.3 SAND

The sand to be used to demonstrate liquefaction has to be susceptible to soil. Which means it should have to following attributes:

1. Fine sand passing 40mm sieve and retained on 200mm sieve
2. It should be cleaned
3. It should be free of dust or silt

To achieve these attributes the sand was first refined through a sieve shaker, with #10, #40, and #200 sieve placed in this order. After that the sample was washed thoroughly. The cleaned sand was then put into the sand tank up to a depth of approximately 18 inches.

In our pursuit to demonstrate liquefaction we used two types of sand; Lawrencepur sand and Qibla Bandi sand. We washed each sand sample, conducted the sieve analysis to obtain the desired grain size and filled the sand tank up to 18" depth.

The Lawrencpur sand did not liquefy due to excessive silt and dust. Depsite thoroughly washing the sand, the dust content was still high enough to allow cohesion of particles and resist liquefaction. The procedure however, helped us arrive at certain conclusions:

Despite thoroughly washing the sand, one cannot be sure about the silt content of the sample. It is therefore advisable to conduct a hydrometer analysis first, to ascertain the silt content. This would give an idea about wether washing the sand would be enough, to remove the silt or altogether different sand sample is required.

4.4 WORKING OF THE TANK

Inside the sand tank wooden sticks are inserted in the sand to depict piles. This would let us study the behavior of pile foundation, when soil liquefies. The motor pumps the water from the water tank to the sand tank above. The inlet valve controls flow of water. The water from the motor, spilts into four branches all heading towards the sand tank.Four inlets are present on the base of the tank. The inlet holes in the base are sealed with silicon and rubber to avoid leakages. The water then hits the porous plate inside the tank; the water pressure gets uniformly distributed across the surface of the plate. The water then rises, countering the effective stress and eventually reducing it to zero,

When the water level equals the top of the sand surface the inlet valve is closed. At this stage, a load is applied to the sand by hitting the outer surface of the tank with a rubber hammer. This load has the same effect as an earthquake would have in real world conditions. The wooden sticks inserted in the soil to act as piles collapse under this load because the sand has lost all its nearing capacity due to excess pore water pressure.

Fig 22: Sieve Shaker

Fig 23: The model in its final form

4.5 IMPORTANCE:

The liquefaction tank is an important apparatus in helping new undergraduate students understand the phenomenon of liquefaction. As described in previous chapters liquefaction can be very devastating both in terms of financial losses and loss of life, therefore it deserves special attention. For this purpose, it is imperative that students have a clear perspective of how liquefaction occurs and which soils are susceptible to it. This model can be of great assistance in this regard.

Secondly this model helps us understand the response of different foundations to liquefaction of soil. In our demonstration, we tried to show piles that were erected in sand and their consequent failure due to liquefaction. Many different foundations can thus be tested.